UNCLASSIFIED

Australian Government

Department of Defence
Science and Technology

A Description of a New Model of Sporadic E for JORN

Robert S. Gardiner-Garden

National Security and ISR Division
Defence Science and Technology Group

DST-Group-TR-3442

ABSTRACT

The morphology and physics of Sporadic E (Es) differs greatly to the normal physics of other ionospheric layers, so it is generally treated and modelled differently. The Es model within the Jindalee Operational Radar Network (JORN) is a real-time model with values based on sounder data, and has essentially remained unchanged since JORN's delivery in 2003 (despite years of progress in sounder processing). While this model can be used to manage the system when Es is present, systemic model difficulties must often be overcome by the manual intervention of experienced operators. This paper describes a new fully automatic data driven real-time model of the morphology of Es, and describes the associated expected propagation characteristic that should reduce the need for manual intervention. It has been adapted to work with JORN ionospheric sounder data in real time and tested with years of data. The models performance is characterised and discussed, and a probabilistic cumulative distribution function (CDF) is used to describe the probable value of the amplitude of Es. It includes an algorithm based on the available sounder data to determine the number of separate Es layers present in the data and a recommendation is made for the new model approach to Es be adopted in any future enhancement of JORN's model of Es propagation.

UNCLASSIFIED

Produced by

National Security and ISR Division
Defence Science and Technology Group
PO Box 1500
Edinburgh SA 5111

Telephone: 1300 333 362

December 2017
AR-017-062

A description of a new model of Sporadic E for JORN

Executive Summary

Sporadic E (Es) morphology and physics differs greatly to the normal physics of other ionospheric layers, so it is generally treated and modelled very differently. The Es model within the Jindalee Operational Radar Network (JORN) is a real time model with values based on sounder data, and has essentially been unchanged since JORN's delivery in 2003 (despite years of progress in sounder processing). While this model can be used to manage the system when Es is present, there are often systemic model difficulties that must be overcome by the manual intervention of experienced operators.

This paper describes a new fully automatic data driven real time model of the morphology of Es and the associated expected Es propagation characteristic that should make the need for manual intervention less common. It has been adapted to work with JORN ionospheric sounder data in real time and tested with years of data. Its performance has been characterised and is discussed.

This model produces a conventional and deterministic estimate of the height of the Es layer (hEs) used in the determination of Es path delay but allows this hEs estimate to have horizontal variations. This model also constructs a probabilistic cumulative distribution function (CDF) to describe the probable value of the amplitude of Es i.e. foEs, at any time or place in the Australian region. This model introduces the idea and possibility that two Es layers may be present at the same frequency and the same time but uses the available sounder data to make this determination.

It is recommended that this new model approach to sporadic E be adopted in any future enhancement of JORN's model of Es propagation.

.

Author

Robert S. Gardiner-Garden
National Security and ISR Division

Dr Gardiner-Garden started life as a scientist with a Bachelor of Science (Honours) from Sydney University in Applied Mathematics (1982) and PhD from Princeton University in Geophysical Fluid Dynamics (Physical Oceanography) (1987). After nearly 10 years as an academinc oceanography he joined Defence Science and Technology Group in 1996 in what was then the High Frequency Radar Division. For the last 20 years he has worked on various aspects of ionospheric and Radar modelling and data analysis focused on understanding and improving the accuracy of Australias Over-the-Horizon Radars.

Contents

This page is intentionaly blank.

1. Introduction

Sporadic E is a layer of free electrons (and corresponding ions) within the ionosphere that is generally transient and irregular in its appearance. It occurs at approximately the height of the normal E region (80–160 km of altitude) and is hence designated the label sporadic E or Es (see Davies, 1990). Es morphology and physics is very different to the normal E regions so it is generally treated and modelled very differently. An Es layer can be highly reflective of radio waves and hence it is importance to high frequency (HF) radar, but its spatially and temporally variable nature makes it notoriously difficult to predict and model. Typically it is a very thin layer of ionisation (only 100 m – 1 km thick compared to the normal E regions 10–25 km) and so its HF propagation properties are generally very different (more mirror like) compared to the other layers of electrons in the ionosphere. There is evidence that the under-lying physics of Es is very different in different regions of the globe i.e. between the auroral region and near the (magnetic dip) equator and in the greater mid-latitudes (5 to 50 degrees South or North) (see Kelley, 1989). For the purposes of supporting the Jindalee Operational Radar Network (JORN) this report focuses on modelling Es in the middle latitudes (5–35 degrees south geographic) and capturing the physics and the behaviour of this mid-latitude sporadic E.

This report is broken into several broad sections. Section 2 briefly describes the existing model of Es for reference. This highlights many of the flaws and weaknesses of the existing model and lays the groundwork for some of the changes proposed. Sections 3 and 4 describe, in overview, the new (simple) fundamental concepts that the author believes are needed to effectively model Es and the new model for Es proposed. This includes an important conceptual distinction between a rigid deterministic model for the amplitude of the Es (foEs) which normally changes rapid and a model of the statistical properties of foEs where the statistical properties of Es change more slowly even when individual realisations (measurements) can change rapidly. Section 5 proposes various measures that can be used to quantify the performance of the algorithms used to describe the behaviour of Es. Section 5 also presents some examples of the performance of the particular algorithms proposed, based on real data. This includes the data from an integrated vertical incidence sounder (VIS) and oblique incidence sounder (OIS) network and separately the observations of Es from the integrated Backscatter Sounder (BSS) network. Finally, there is some discussion in Section 6 concerning a proposal for how the human operators could interface with these algorithms in order to catch examples of poor performance and simplify the algorithm options for easier operator interpretation in order to improve the overall Radar performance experience.

This report does not address in detail the original sounder processing that turns each single sounder observation or measurement from the Es region into a local parameterisation of the true height i.e. hEs and foEs parameter estimates in the case of VIS or OIS sounder data. These parameter estimates (including some assessment of the measurement quality) are the raw inputs to the modelling process and are described in separate documents concerning the raw VIS, OIS and BSS processing.

2. The Existing model

The existing Es model integrates sounder Es parameter data produced from each of the VIS, OIS and BSS sounders into a single single-layer and network wide model for Es. This model can be thought of as having 3 separate elements, describing the 3 different Es parameters hEs, foEs and fbEs. These are presented schematically in Figure 1 below. Unlike the other ionospheric layers, the thickness of the Es layer (yEs) is not a dynamically assigned parameter. This means the Es layer can be thought of as a simple thin mirror. Frequency dependent retardation resulting from a partial penetration of the Es layer is seldom observed though retardation within the Es return can be observed as HF rays propagation through the normal E layer prior to reaching the Es layer. This delay from underlying electrons results in the virtual height of delay to the Es layer (vhEs) being potentially different to the true height of the electrons i.e. hEs though often they are treated as the same value.

For the first element of the modelling exercise (modelling hEs), all the VIS and OIS sounder height data (without regard to location) is included to estimate a regional representative value for hEs(t) that varies with time. Temporal smoothness in this height estimate is produced by deriving a hEs estimate based on the last 30 minutes of sounder parameter data.

$$hEs_{estimate} = mean(set\ of\ observations) = \ 1/N \sum_i (weight * \ hEs\_observation) \qquad (1)$$

New real time ionospheric model (RTIM) updates generally occur every 10 minutes so that a considerable fraction of the data is usually unchanged from one estimate to the next. The details of how the existing algorithm filters out bad data are left for another time. The result of this algorithm is that the code generates a single spatially uniform estimate of hEs for each RTIM update. An additional single measure of the spread of these samples (a measure of the sample standard deviation, σhEs) is also manufactured to characterise the height estimation uncertainty.

The second element of the modelling exercise (modelling foEs) is based on all the VIS, OIS and BSS sounder raw estimates of the parameter foEs. In the OIS case these estimates are applied to the model at the OIS path mid-point. The BSS sounder also has the potential to generate an indirect estimate of foEs. This starts out as an estimate of the maximum observed oblique MoF_Es in a given BSS beam at some range. This MoF_Es is then converted to an estimate of midpoint foEs using the value for hEs (established earlier) and an equivalent mirror model for propagation. In the case of the current system only one single value of foEs is estimated from each BSS beam at a pre-nominated range (1600 km) or at a range nominated by an operator. These are the raw foEs estimates, at a limited set of places, which go on to be used to estimate foEs at each and every RTIM grid point.

The highly transitory, temporal nature of Es is accounted for within this model by only using the single most recent sounder observations of foEs from each sounder source when estimating the specific deterministic value for foEs. The highly variable spatial nature of Es is accounted for by first dividing the geographic coverage up into a number of sectors and testing each sector for containing foEs data that is either ''on'' or ''off''. If some current Es data is non-zero in a given sector then the Es state of that sector is set to ''on'' and all data within that sector is then used to produce a spatial map of foEs within that sector. Some algorithmic complexity is produced by grouping adjacent sectors that are both 'on' into an enlarged group of sectors prior to the spatial mapping of foEs. The original sectors are divided up on the basis of the Radar FMS beams (one inner sector and one outer sector for each FMS beam). Because the map of foEs is driven by data from a limited set of positions (the positions of the VIS, OIS and BSS midpoint samples) the modelling needs to use this irregularly spaced input data to estimate foEs on a regularly gridded map of foEs at each RTIM update, within any 'on' sector. The details of how this algorithm filters out bad data, manage overlapping BSS sectors and map foEs within a group of sectors are left for another time. The core algorithm is based on finding a mean of all the data within an 'on' group of sectors and using that as a background everywhere in the sectors and then Kriging (spatially mapping) the difference between the data and its mean to establish a final foEs estimate everywhere (at all RTIM grid locations) within an 'on' sector and ultimately within the RTIM grid. The key point is, this method produces a map of foEs that is spatially and temporally quite variable and there is little inherent smoothness or continuity in the derived foEs map.

The third and final element of the Es modelling is the generation of a spatially and temporally varying estimate of fbEs that is needed in order to calculate both the path loss on oblique returns from the Es layer and to represent the degree to which underlying Es will obscure propagation through the Es layer and into the ionosphere above. In the existing Es model this fbEs is just assigned to be a simple single constant fraction of the estimated value of foEs (i.e. fbEs = αfoEs) and hence it is not recorded as an additional parameter field within the RTIM. The parameter 'α' is used to control the path power loss estimated on propagation through paths that are above (or through) the Es layer but the parameter 'α' may or may not also be used to estimate the loss of the Es layer tables themselves depending on the part of the system where the algorithm is applied. At present the value of 'α' is set to a value typically between 0.5 and 0.8 consistent with values observed in Sinno et al (1976). There is a potential for a time of day dependence in the assigned value of 'α'.
Note: It is worthwhile to note that there is a potential for a difference between the frequency where transmission and reflection losses are equal (faEs) and the frequency of fbEs where reflection is effectively total (and transmission losses are high).

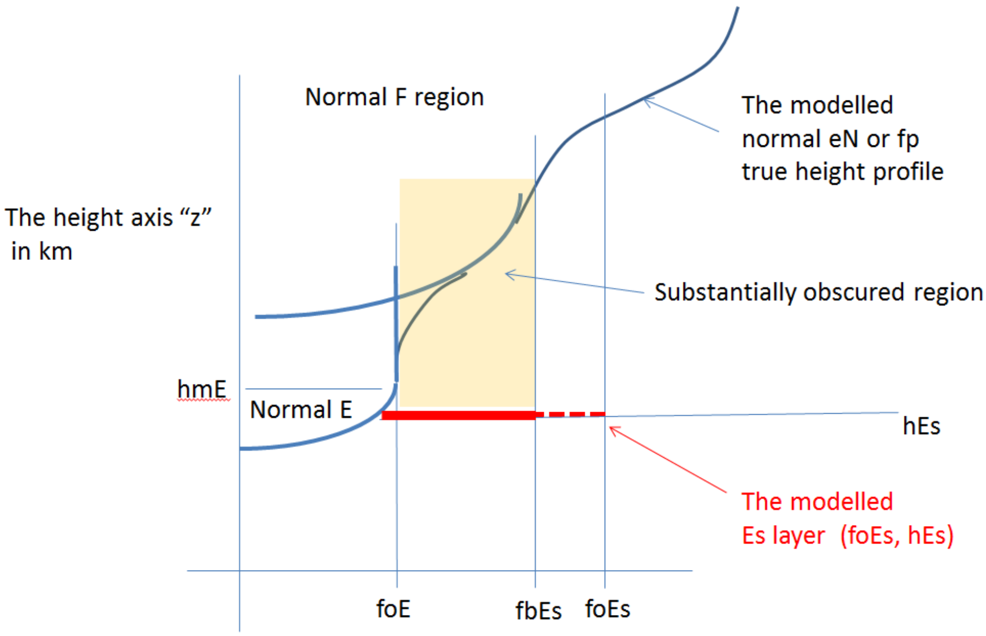

Figure 1 A schematic of a plasma frequency (electron density) profile versus true height with a single Es layer described by parameters hEs, foEs and fbEs.

3. Some Basic Physical Concepts

The existing model of Es is a deterministic model that supposes a single value for each parameterised property (and potentially a small Gaussian distribution of error in the estimate of that property). This model assumes every single measurement is accurate and of physical origin, and multiple sounder measurements are cross-consistent (without making any attempt to reconcile potential differences between the different types of sounders). The sporadic nature of Es is then used to justify each single estimate changing substantially and rapidly in space and time. This creates a disconcerting level of Es variability in the model that is not always consistent with a more general view of the sounder data or the operators experience with the Radar.

The general goal of this new model is to adopt a more physically reasonable conceptual model of Es and hence produce a more accurate model able to integrate Es data from multiple sources. The model adopted does not use a single deterministic value to describing Es at an instant in time and space but instead uses a probability distribution of possible values to describe Es in a given region of time and space (given a frequency). This characterisation of Es (as having a potential distribution of values) is like modelling the possibility of intense thunder storms in a given place and time, that is, it offers the possibility that the large scale properties of this distribution will change slowly and predictably and be more consistently in space and time even if the individual measurements or observations upon which the distribution is based are highly variable. The intent is to be less definitive but more trustworthy and reliable in a statistical sense. Specifically the goals of the new model are to:

- generalise the existing model of Es away from specific deterministic conceptual model towards a description of the likely distribution of Es
- make the modelling assumptions and limitations clear
- adopt scales and sample sizes so that model estimates of the distributions of data are generally driven by large sample sizes
- reconcile in a physical way the consistency and potential inconsistency of different sounder measurements of the same region of space and time and
- implement the model in a careful fashion (with automated checks and balances) so that at the end of the modelling process the model is both consistent with all the input data and with all the modelling assumptions.

It is proposed (and will be demonstrated) that this new model is a smooth and consistent match for the environment within which the Radar is operating as well as a statistically consistent match to the sounder data. In order to achieve this, the model must reconcile the various sounder measurements of foEs from different instruments and times. To do this a conceptual model of the impact of Es on sounder measurements described in Figure 2 below. This is the same as the ‘cloudy Es’ conceptual model proposed by many physicists studying Es (see Mathews, 1998 & Barnes, 1995). With this model, if a peak value of foEs occupies 10(1)% of the sounders sampling footprint (with this fraction of the region covered) it is expected that the amplitude of the peak Es returns will be 10(20) dB lower than the value observed if the layer was saturated. This 10(20) dB loss value is the detection threshold that should be adopted by the Es sounder processing if the raw sounder processing is to be consistent with the way the data is used. Similarly, if a background value of ionisation covers 90(99)% of the sampled region of returns then propagation going through that region will suffer a 10(20) dB loss when trying to penetrate the Es layer and reach the layers above.

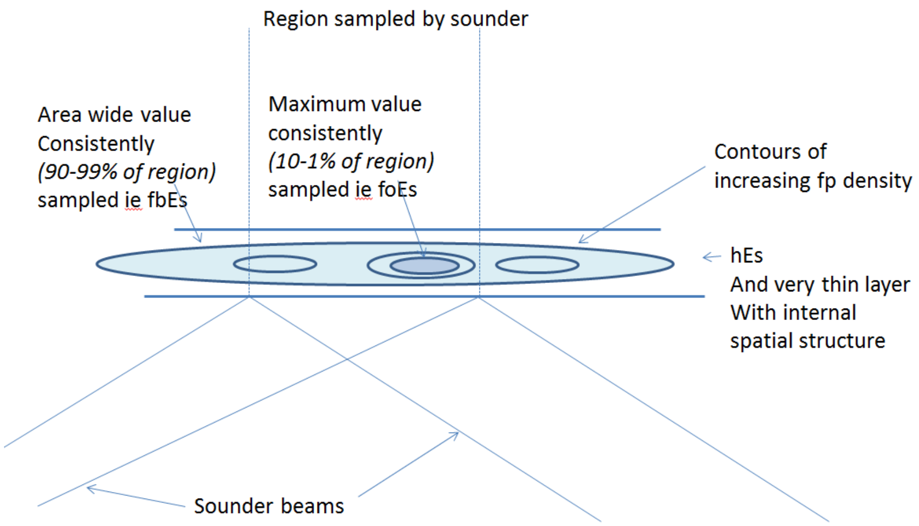

Figure 2 A conceptual schematic of a sounder sampling a 'cloudy' region of Es.

To characterise the distribution of Es in a geographic region the model algorithm needs to define a region that is large enough to normally accumulate a significant number of measurements but small enough to allow spatial and temporal variations to be represented. For the case of the JORN sounder network the algorithm has adopted a weighted data accumulation scale of 2-3 degrees in size. Assuming a potential for horizontal drifts of ionospheric structures on the scale of 100 km/hr then over 30 minutes of a data collection the individual measurements might be expected to change but the distribution of Es that is characterising the region (and time) is expected to remain a meaningful average.

The ionospheric footprint of a single VIS or OIS sample (integrated over a time of minutes) is typically <5–10 km. Within a region of 100–200 km square, the 'cloudiness' of foEs can be expected to cause successive Es measurements (within a 30 minute period) to be substantially different. If this physical interpretation of Es is correct then it can be expected that successive individual VIS and OIS samples (5 minutes apart) will be essentially independent samples within the distribution of Es (describing Es on the scale of 200 km and 30 minutes) as the instruments sample different small cloudy patches of the sky. Hence, many measurements can be accumulated to describe an areas characteristic or cumulative distribution function (CDF) rather than each measurement being used deterministically to characterise a highly variable set of individual samples. An example of this method of producing and describing a CDF is presented below in Figure 3 where p_fX is the probability Es will be observed at or below frequency X and f_pY is the frequency above which Y percent of the Es occurs.

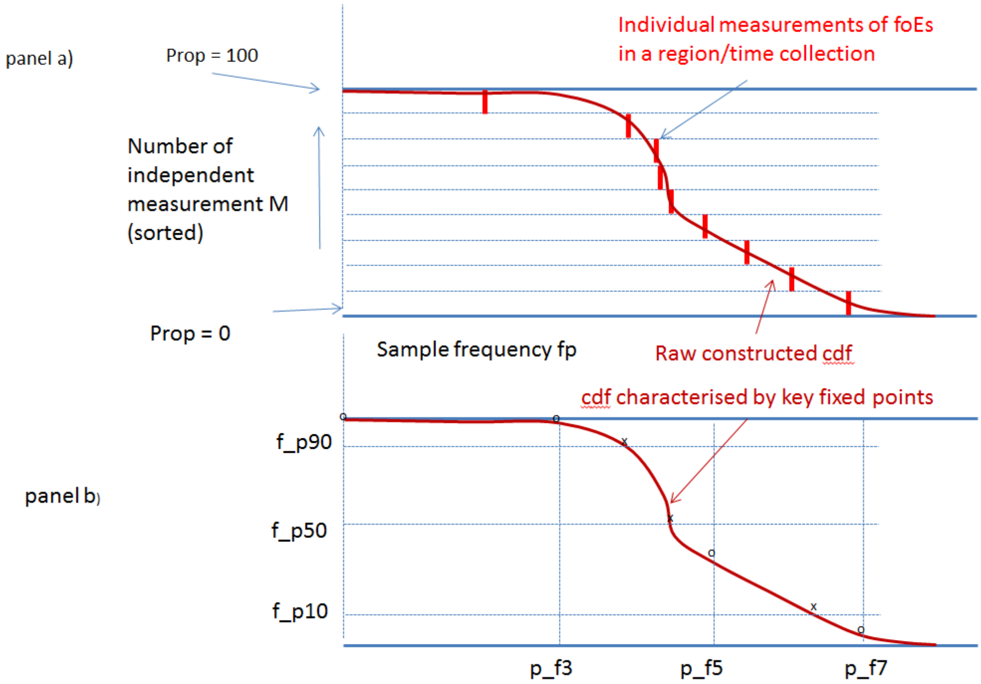

Figure 3 A conceptual schematic of an accumulation of multiple sounder measurements of foEs (a) producing a cdf of foEs and (b) the derived cdf with characteristic fixed points (f_p10, f_p50 ,f_p90 and p_f3 p_f5 and p_f7 MHz).

Maps of foEs (p_f7) for summer and non-summer months have previously been presented by Smith, E.K., 1978. Maps of the frequency at which different probability densities are met (i.e. f_p10, f_p50 and f_p90) or maps of probabilities at different fixed frequencies (i.e. p_f3 p_f5 and p_f7) from this model all contain useful information. At present it is unclear if this distribution function should be simply characterised by empirical parametric function based on a limited set of parameters or if a more complete discrete picture of the frequency dependent shape will be required. Current versions of the code maintain a complete description of the distribution function but at some point it is expected to reduce this to a simpler and more limited form.

A second basic physical concept that is poorly handled within the existing model is the difference between a bad observation and a sample that has measured no Es. If missing measurements of Es are treated as foEs=0 then, potentially, a large amount of flicker can be introduced between periods and places where there is a large and observed value of foEs and adjacent periods or places when it is spuriously estimated to be absent (zero). Examining this more carefully suggests that 'no measurement of foEs' does not always mean 'foEs = 0' but it can mean that a valid measurement of foEs was not possible. One common reason is that some part of the frequency range was effectively excluded or obscured from the sounder sampling process. The question thus is; how should this information be used in the foEs modelling process?

The physical assumption about Es adopted in this new model of Es is:

> if the Es is obscured then the true value of foE is 'equally likely' to occur at each and every frequency below the observed instrument obscuration frequency fB

Estimation of the new variable quantity fB has yet to be discussed but it is worthwhile to note that it is different to obscuration frequency fbEs. fB is a property easily estimated (or estimate-able) for every sounder run even when no Es is measured. The obscuration of Es within a sounder measurement can be the result of a lack of power (gain) in the OIS path, that is, and inability to measure down -20 dB or it can be the obscuring effect of the normal E layer or the obscuring effect of the BSS F returns. How to estimate a value for fB is left for a later part of this report. Without other information the best that can be assumed is that there is a uniform probability of foEs in the range [0: fB] This means each blocked or obscured measurement of Es acts as a wedge in the accumulation of a measurements used during the construction of the cdf to describe foEs. This wedge effect is presented below within Figure 4.

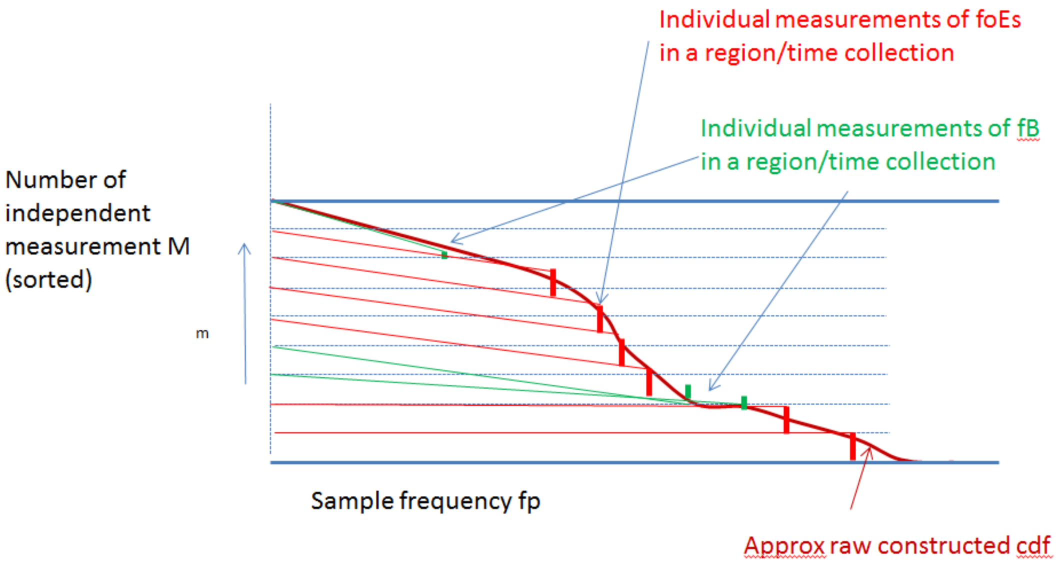

Figure 4 A conceptual schematic of multiple sounder measurements producing a cdf of foEs including measurements with no visible foEs (but a blanketed frequency fB).

Instead of using a normal distribution, it would be desirable to use the independent estimate or climatology for the distribution of foEs in order to make a better estimate for the distribution of foEs when no observation was available. However, while this approach appears superior it is also much more complex and hence is left for another time. Also, the accumulation of a cdf as presented above does not account for the possibility of different measurements having different weights but that also is left for the code itself. These two main ideas (foEs as a distribution of values and missing measurements of Es being treated as unobserved Es) represent the core of a new method to understand and model Es where the challenge is to construction a CDF describing the likely and most likely value of foEs from real data.

A third basic conceptual change in this new model is derived from looking at a great deal of good quality Es data and recognising that while the intensity of the Es layer (foEs) may be quite sporadic, the height of the Es layer is much more consistent. More-over, the height of sporadic E layers can be described as falling into two distinct groups:

1. high layers of ions descending over time (sometimes referred to as Tidal ion layers or descending layers)
2. lower layers that are more variable but are consistent with the traditional conceptual models of residual Es (i.e. material existing as the left over residual after a descending layer has stopped descending), see Haldoupis et al , 2004 & Haldoupis ,2012 for early discussions.

Conceptually these two components of Es are often distinct and separate. To produce an accurate model of Es height (and delay) it is desirable to model the possibility of one or two separate Es layers existing simultaneously i.e. make this conceptual height difference explicit. Keeping track of two separate layers is easy when observations are numerous and the layers are well separated but it can be more difficult when the two Es layers are inseparable because of limits in the measurement process (Es is then represented as a one single joint Es layer). Accounting for this variation requires a flexible model to be based on a data driven decision to transition from two separate layers to one combined layer on a case by case basis. Many adaptive algorithms have been tried and tested, for example, a k-means approach. Exactly how this height grouping and separation is achieved is discussed in later sections.

It is our observation that these two layers can exist simultaneously and the apparently higher layer is not generally the result of off angle reflections (much delayed) but is just a separate higher layer. This interpretation is supported by direct measurements of angle of arrival on a limited set of OIS paths during the ELOISE trial (work not reported here).

Sample number density maps based on a large number of hEs measurements (with greater than 1 million samples) show the typical or climatological pattern of hEs. Figure 5 below shows an example of this hEs diurnal climatology versus hour of day based on data from sounder sites in the Australian region. This summary of hEs data shows that regions of high and low Es can be separated using a simple fixed time varying curve (starting at local dawn around 110km and descending to 95 km by the next cycle) as a separator. This curve is called hEs_sep(t). It is actually a curve based on UT time and the solar zenith angle (chi) and hence more correctly is hEs_sep = fn{t; doy, X, Y}.

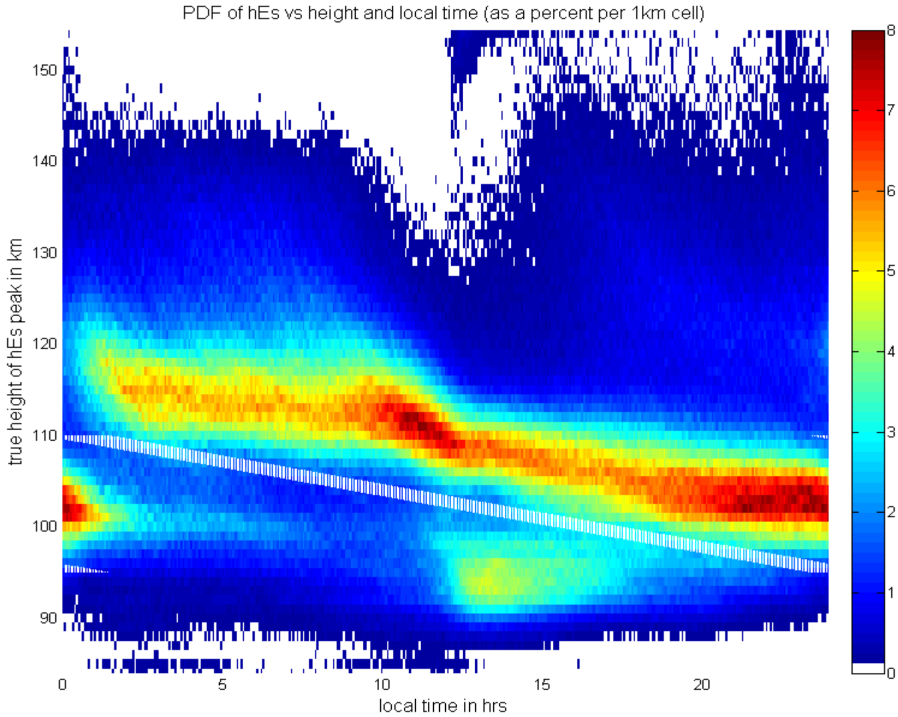

Figure 5   An area and day averaged and normalised pdf for hEs presented as an image of the number density verse height and local time of day. This is based on all JORN VIS & OIS measurements of hEs over 1 year (2016). Over-plotted (the white lines) are the positions of the model hEs-separator between high and low Es for all the sites and days.

This observed distribution of hEs data leads to the belief that, to achieve a more accurate model of hEs, a new model should allow hEs to vary in both space and time and (when the data demands it) allow the model to admit the possibility of two separate layers existing at different heights simultaneously.

The final (fourth) simple concept highlighted in this new model of Es is that while the true height of an Es layer is hEs and the layer might be mirror like, but this does not stop the apparent virtual height of the layer vh_Es from being greater than hEs. This is because a possibility exists for retardation within a sounder measurement from propagation having penetrated the underlying normal E layer. This additional retardation is strongest at the low frequency edge of propagation as freq -> foE. The new model accounts for this concept within its utilisation of hEs data from the various sounders because, while vh_Es(f) is often the actual original measurement, hEs is the sounder processing output used as this models input.

4. Details of the New Model Algorithms

The purpose of these new model algorithms is to construct a spatially variable estimate of foEs and hEs at all places and times. The input for this process is the raw sounder data and the principles adopted and discussed in the previous section. The basic strategy adopted is to use a weighted sum of all nearby data to construct an estimate. The details are discussed in this section and includes a discussion of:

1. how to detect and eliminate bad data
2. how to select and define the sample sizes and weights and the implied decorrelation scales for this weighted averaging process
3. how to reconcile the differences between data from different types of instruments.

The following subsections will discuss the details of all the key modelling algorithms and focus on explaining the approaches to addressing each of the above challenges. The following algorithms are dependent on a sample of the most recent 30 minutes of sounder data (dT= 30 minutes) from the entire network being available. Typically this is 4–8 samples from each single VIS site or OIS path and most likely 4–6 Es traces from each BSS beam. Algorithms could adopt a shorter dT but this inevitably would result in less data being used to make an estimate and hence a more highly variable model estimate.

The sample weight function adopted in these algorithms is the simple functional w_ij = 1/(1+dist_ij^2) where dist_ij is the scaled distance between the data sample i and the test point j. In order to accumulate a significant number of VIS & OIS data samples at all the grid points of interest in the Australian region the algorithms, adopts a distance scale length of 3 degrees i.e. data 3 degrees away from a target site will have weight = 1/10th that of the weight from a single sample exactly at that location.

Figure 6 below shows the weighted sample number density typical of the JORN sounder network of Es inputs if all data was available. Typically only 40-80 % of soundings will have some hEs data so this leaves some times and places with very little data available. The threshold adopted is <16 sample points contributing to an estimate results in that estimate being considered unreliable. The sample density of data available from BSS soundings is also presented here though this can only impact the foEs estimation and mainly in those circumstances when foEs is observed in front of the BSS F layer leading edge.

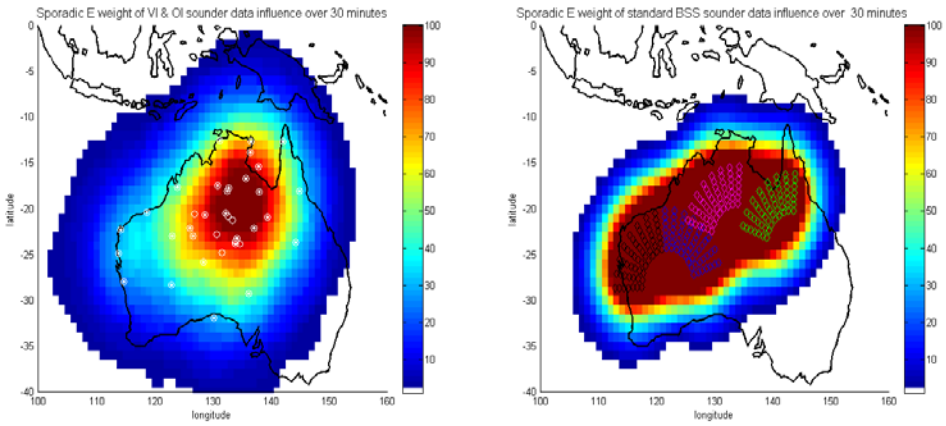

Figure 6 A map of the maximum possible weighted number of samples available for Es parameter estimation (when the temporal accumulation interval is 30 minutes and when data from all sounders is available) a) from the JORN VIS and OIS sounder network and b) from the JORN BSS network.

4.1 Height hEs

Only the VI and OI sounder data contains direct information about hEs. The observed true height parameter data hEs is recorded from each VI & OI sounder within the sounder data archive. This new Es model algorithm processes the hEs data within three stages.

The first stage gathers all the sounder data within the dT group and applies the various small instrument bias corrections so an unbiased input dataset is available. Part of this process is to only accept hEs data from OIS paths with ranges < 1850 km so that the very long and low elevation paths do not contribute to the system hEs estimate (and potentially bias a final estimate).

The second stage of the hEs processing constructs an unweighted regional average for hEs from all the data deemed good (called hEs0_ave). This stage also uses the hEs separator line described in Figure 5 to separately flag high and low Es data (with some overlap) into two separate groups and hence creates an area averaged estimate of the low and high hEs (called hEs1_ave & hEs2_ave). To cope with the potential of little data being present at some time this averaging is regularised by always including a reference value with a small weight i.e.

$$hEs_{estimate} = (\sum_i hEs_{obs_i} + \gamma\ href)/(N+1) \tag{2}$$

The value of *href* adopted is,

href = hEs_separator +5 km for hEs0 ,

href = hEs_separator - 5 km for hEs1 and

href = hEs_separator +10km for hEs2

This regularised fit to the available data assures that the model will always be able to produce an hEs estimate. Schematically, these 3 overlapping groups of height samples (high, low and combined groups of data) are presented below in Figure 7. Each group has a mean and standard deviations. Dawn is a moment of substantial change in the separator line and occurs at different times at different locations. This produces substantial change in each of the high and low Es models. This results in the high and low estimates of hEs being more likely to overlap around dawn. The standard deviation estimate also allows the flagging of poor quality data prior to the next update, that is, data that is grossly inconsistent with its neighbours. Poor quality outliers are identified as points which are > 3 sigma away from the mean of any of these models when the mean has significant data samples available. This results in the outlying hEs value of an observation being the principle cause of any particular observation being labelled spurious (entirely inconsistent with respect to numerous neighbours). Individual inspection of ionograms suggests this is most commonly occurring when the automatic scaling process latches onto a long lasting meteor and spuriously reports it as an Es return. Sometimes (temporarily) true hEs data will be falsely labelled as outliers and excluded if a weak new layer of Es is present and an old dominant layer has yet to die away. Later analysis will show this is not common.

After this processing, a site independent estimate of the height of Es (hEs_ave) is now available to be used as a fall back reference for the spatially variable map (used when insufficient local data is present). It is also noted that the single joint unseparated estimate of hEs (hEs0_ave) is very similar to the previous systems final hEs estimate. To smoothly manage the estimation of hEs through periods of no (or very little) data the regularisation term in the weighted sum of data (weighting the solution back to predefined reference values) was introduced. This will only affect the value of the hEs solution when the number of good samples is very low.

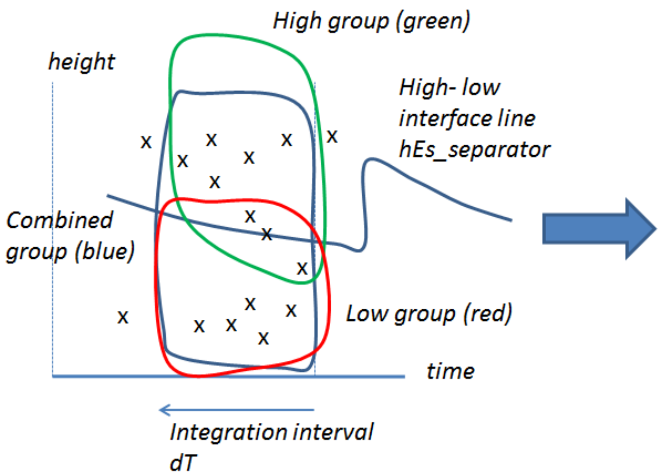

Figure 7 A conceptual schematic of multiple sounder measurements producing a cdf of foEs including measurements of no visible foEs (but a blanketed frequency fB).

The third and final stage of the hEs processing is to now estimate hEs at each grid point (generally the RTIM grid points but points selected could be the sounder sites themselves if the purpose of the calculation is to do analysis of the model compared to the original data). This excludes points labelled as outliers in the earlier stages of processing. By producing a weighted average of all observations surrounding any particular point (weighted appropriately by quality and distance) and having the background spatially averaged estimate of hEs the modelling of hEs is completed. This algorithm inherently cycles through or processes in parallel each RTIM grid point location after creating appropriate distance dependent weights between each target location and the input data sites.

An example of the raw data and the area averaged estimates of hEs0_ave , hEs1_ave & hEs2_ave (and their corresponding standard deviations) based on sounder data from a period in 2016 for a 5 day period is presented below in Figures 8.

An example of the raw data at a single location 'i' (and the spatially local estimates of hEs0_i, hEs1_i & hEs2_i and their corresponding standard deviations) for the same 5 day period is also presented below in Figures 9. In this case, the location used for this example plot is arbitrarily selected and is the OIS path Kalkarindji to Mt Everard i.e. an OIS midpoint in the middle of the sounder network.

In Figure 8 there are hundreds of data points densely packed under the display of the estimated hEs curves, so, while it may appear that numerous raw data points are flagged as outliers, the number of outliers is actually only a small percentage (<2-5%) of the total dataset. Also, while Figures 8 and 9 clearly present significant trends and patterns in the day to day variability of the descending hEs layers observed, the purpose of this paper is to report on the Es modelling method and its performance and so discussion of the observed morphology of hEs and foEs is left for another time. Never-the-less, it is worthwhile to note that these Figures clearly show that separating the model of hEs into two separate layers clearly gives a superior representation of the data at particular periods of time (like around 216.5 and 217.5 and 219.5).

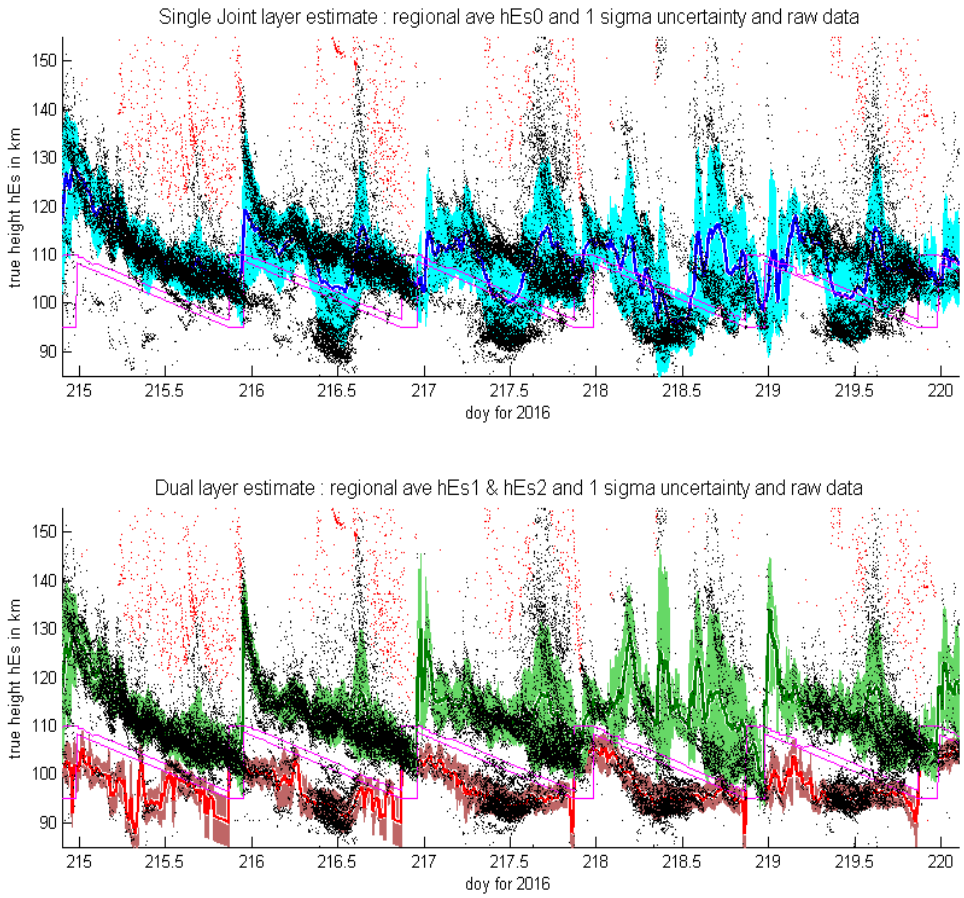

Figure 8 *hEs data (black dots) and the corresponding high (green) and low (red) and joint (blue) area averaged estimates of hEs and their standards of deviation from a 5 day period in 2016. Data identified as outliers are over plotted with red dots. The magenta lines represent the high and low limits of the hEs_separator curves from each sounder location and time.*

In Figure 9 below, there are clearly times when the volume of Es height data near the particular location (within 3 degrees) presented is low or absent. Never-the-less, the hEs estimate persists because data is available at nearby locations (not presented directly on this Figure) or the solution has relaxed back towards the spatial average estimated height.

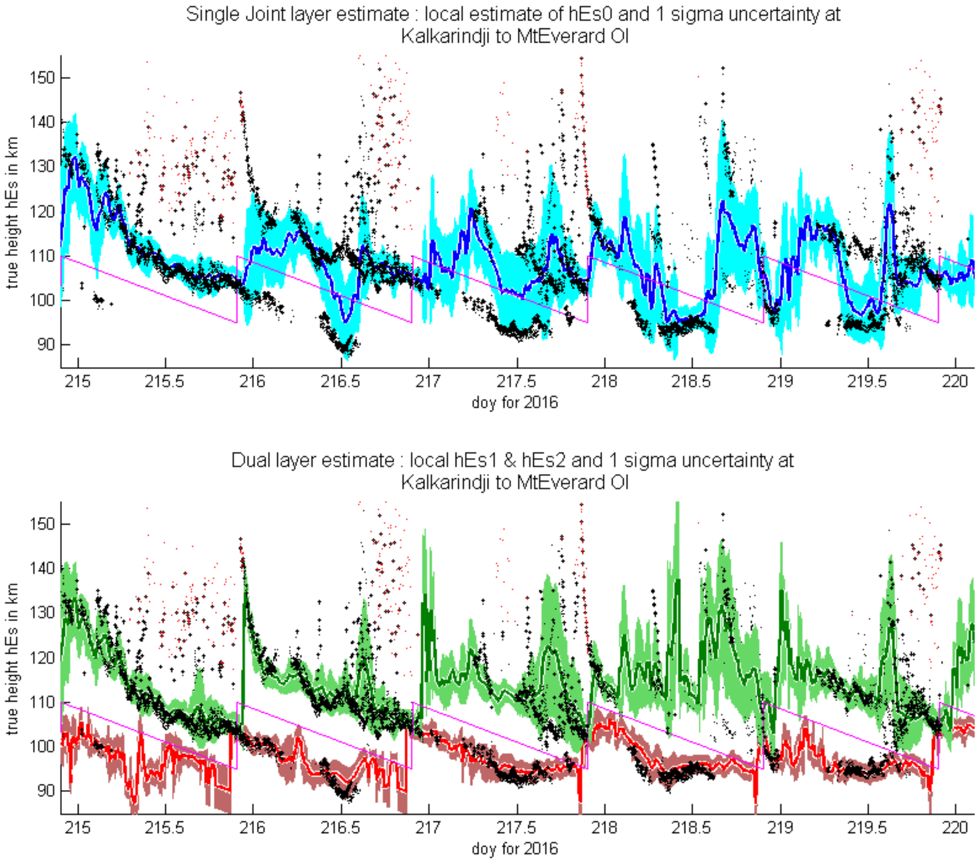

Figure 9 *Good hEs data at a single site (black dots) and the corresponding high (green) and low (red) and joint (blue) estimates of hEs in the vicinity of a single OIS path mid-point and the associated fitted model standards of deviation from a 5 day period in 2016. The magenta line represents the hEs_separator curve at this location.*

4.2 The Number of Separate Layers: nL

In order to capture those circumstances when multiple Es layers are present and distinct and contemporaneous, the new model of Es introduces the concept of supporting the separate existence of either 1 or 2 Es layers being present at a given time and place. This is characterised by a new variable parameter nL meaning the number of separate Es layers. The modelling challenge is hence to estimate nL at any given place and time and account for those times/places where nL = 1 or 2. In the following section the algorithm used to estimate nL is described. Many different algorithms where trialled and tested (for example, adaptive k-means approaches, but, in the end, we adopted the best performing and simplest option. A related challenge is to decide what to do when there is either very little data or the data is so poor or indistinct so that a distinction between a single-layer of Es versus a two-layer model of Es is difficult to make. The core purpose of this updated model is to improve the accuracy (reduce the uncertainty) of the modelled Es path delay by allowing more variation within the model of hEs (when the data supports it). While the default should always be the simpler case i.e. one single joint layer of hEs, sometimes the modelling preference is for temporal continuity i.e. if data supporting the existence of one layer runs out should the algorithm let the layer status persist? Balancing simplicity and temporal continuity is just one of the modelling decisions behind the choices in the algorithm.

Some modelling (algorithm) design considerations are;

1. Under what conditions is it best to switch to describing the system as two separate layers (rather than just one)?
2. How can the algorithm assure that the estimate does not flicker between a one-layer and a two-layer description of Es?
3. Is it desirable to have the nL change between 1 &2 layers over all space simultaneously (on the bases of the area averaged data) or is it desirable to have nL= 1 |2 to change on a spatially local basis?

Looking at typically accumulations of hEs data it is observed that the volumes of low hEs data (data with heights below the external hEs separator line) can be quiet sparse and sporadic and so it is easy to start by answering the third design question first. If the choice of nL=1|2 is going to be based on significant amounts of data then the algorithm decision about nL must be based on the area averaged volumes of data and hence the algorithm adopts a common nL=1|2 across the entire domain. Because the main purpose of this model is to support JORN and model Es in the Australian region (not the entire globe) this simplification is a tolerable restriction.

Following this decision, there is now a need to examine the area averaged properties of the data to establish how to determine if two Es layers are distinct and well separated (and nL=2) versus the two Es layers are indistinct and overlapped (and nL=1 is the best choice). The criteria adopted by the model algorithm are described below.

Firstly, at each new time, the algorithm addresses the case when there is significant data (>16 good samples) in both the regions high and the regions low layer at this time. This means that a determination of nL based on data is possible and should be straight forward (and the regularisation condition has had little effect).

If $hEs2- \sigma hEs2 >> hEs1+\sigma hEs1$ (3a),

then the two layers are well separated and nL can be safely set to 2.

Alternatively,

if $hEs2- \sigma hEs2 < hEs1+\sigma hEs1$ (3b) then the two layers overlap and are not readily able to be separated and data suggests nL should be set to 1.

Practical experience has resulted in the >> inequality of equation 3a being assigned a gap threshold of 5 km (though numerous other conditions were trialled). The more statistically common test of sep_value = (hEs2-hEs1)/ sqrt(σhEs1^2 + σhEs2^2) <> threshold was found to be quiet jumpy and in need of a difficult to argue for hysteresis in the setting of the threshold.

This initial phase of algorithmic testing handles many cases but excludes two cases,

1. where the high and low layers are close to overlapping (the separation is less than gap threshold or 5 km apart)
2. where there is insufficient data within a layer.

In Case 1; If there is a significant number of good data points in both layers but the two separate layers are close to overlapped then there is a potential for jitter between nL=1|2. This can be addressed by introducing a small amount of hysteresis into the algorithm. This hysteresis is achieved by following the following instructions when determining nL:

if gap < 5 km and previous nL =2 then persist with nL=2 (until gap is zero) (3c)

Alternatively,
if gap < 5km and previous nL =1 then persist with nL =1 (3d)
(until layer separation is well clear i.e. gap > 5 km).

Because the background estimate of layer height changes slowly, bridging the 5km gap in hEs normally takes some time and in this way this algorithm introduces stability and hysteresis into the hEs estimate.

The final case that needs to be address is the second case referred to above i.e. the case when there is insufficient data to be sure of any partition. In this case the algorithm adopted is:

if a high layer has significant points and is well clear of the climatological interface then continue to call this data high (nL=2) even if the lower layer (with few points) overlaps. (3e)

Similarly
if a low layer has significant points and is well clear (low) of the climatological interface then continue to call this data low (nL=2) even if the higher layer data (with few points) overlaps (3f)

If either layer is dominant in numbers and laps or is close to the climatological divide (the separation interface) then declare nL =1 (3g)

Finally, if there are few points in both layers, if nL starts with a value nL= 1 (the previous estimate) then persist with nL=1 that is one layer. Alternatively if nL starts with a value nL=2, two separate layers then persist with two separate layers, all other things (previous rules) being equal. (3h)

This completes the assignment of nL for all possible cases (starting with a historical default of nL =1)

This value of nL =1 or 2 will vary over time as the data changes and is used in subsequent parts of the model to determine which of the previous hEs estimates is put to use within the model of hEs. An example of the result achieved by applying this algorithm is described in Figure 10 below where the top panel is the area averaged hEs estimate and the bottom panel is the hEs estimate at a single site.

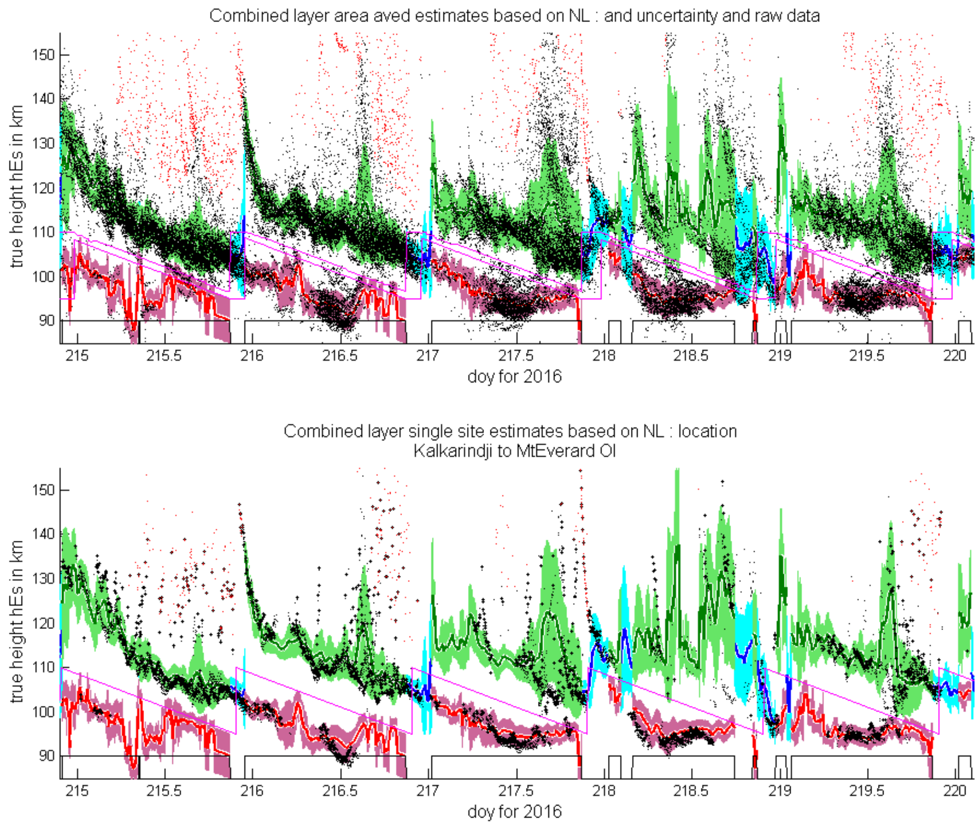

Figure 10 (a) The hEs area averaged data and fitted results corresponding to Figure 8 where a curve of nL parameter switching between 1 layer and 2 layers is overlayed in the bottom of the image and (b) The local hEs estimate fitted at a single site corresponding to Figure 9 after nL is applied to switch between the common hEs model and the two simultaneous layers.

In this sample of data the transitions from nL=2 to 1 and back again can be observed. It is very common to have transitions at the end of the day and the start of a new day because during this period the region of samples labelled both high and low simultaneously is large (because the dawn terminator is dividing the domain) and hence overlap between hEs1 & hEs2 is more common.

In addition, the data in Figure 10 presents some days of the year where the high and low Es are well separated for most of the day and other days of the year when the high and low returns are essentially indistinguishable and hence the Es model has adopted is single joint layer grouping (blue). Analysis of the typical performance of this nL selection algorithm is left for a later section of this report. The overall suggestion is, this algorithm has assigned an actionable and interpretable pattern to a highly variable dataset.

4.3 VIS & OIS Based Critical Frequency: foEs

The foEs modelling exercise starts by being based on the VIS and OIS measurements of Es (where the measurement quality flags are determined from the hEs measurement). In the same way as the hEs data, the foEs data is grouped into high and low and joint groups. To estimate the properties of foEs, the algorithm must again constantly maintain three groups of samples 0, 1 & 2 (for the cases of one joint or two separate layers) and use the nL assessment to determine which group properties to use within the final RTIM estimate. A key to the estimation of the CDF for a group of foEs measurements is, How does the system interpret and use a valid measurement that has failed to observed any foEs? This centres on developing a method for the estimation of a blanketing frequency fB (discussed in the previous section) for each of the instruments based on experience with the data.

Number density maps of data sample density vs foEs and hEs from many VIS sounders and many days (millions of samples) are presented below in the left hand panel of Figure 11. This shows that successful foEs values are rarely observed below 1.2 MHz in these particular instruments. Adjusting and replotting the same data so the horizontal axis in the plot is δ foEs (ie foEs minus the normal E layer foE climatological value foE_clim) rather than just foEs and a slightly different picture becomes clear. The right hand panel of Figure 11 shows that while foEs is not commonly observed below the value of foE_clim it can occur if the hEs height is below the normal E returns. This plot enables a visualisation and estimation of the gap foEs must be in front of normal foE in-order to be reliably observed within a VI sounder image. This data suggests that high Es returns are seldom observed below foE + small gap and low foEs returns can sometimes sneak in at lower heights but are generally excluded by the sounder equipment and processing if the frequency is below an absolute threshold of 1.2 MHz. These observations have resulted in the production of a simple model for fB applied to every valid sound run (those with foEs data and those without) such that

fB (high)= max (1.2, foE_clim +gap)
where the gap is typically 200 KHz (4a)

and

fB (low) = max (1.2, .9*foE_clim) (4b)

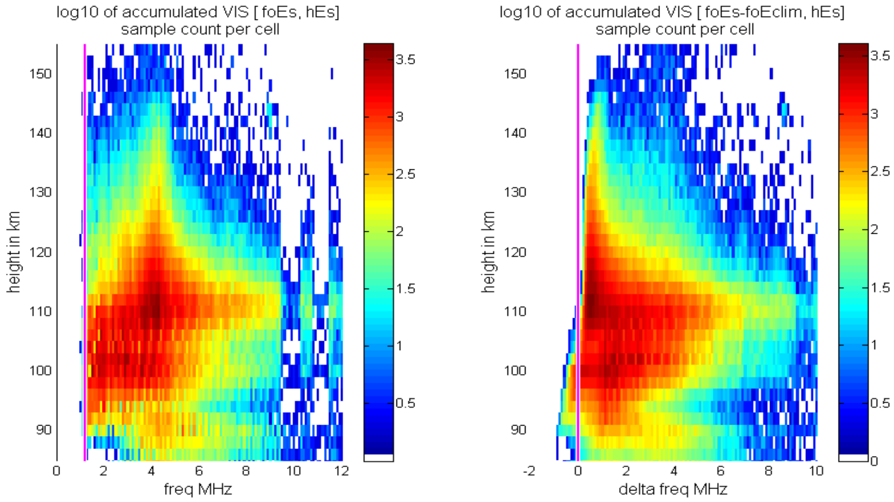

Figure 11 (a) Number density map of log10 of the binned sample count for foEs vs hEs data from all VIS sounder data from 2016 (b) the same data as panel (a) but with the x axis changed to δfoEs where δfoEs = foEs-foEm ie the foEs wrt the climatological model of normal E.

A similar sample density image of OIS data converted to the vertical (Figure 12) shows the additional sensitivity down to lower frequencies compared to the VI sounder data but basically the same functional pattern. This suggests the concept of fB>0 is particularly important to understanding Es at night and reconciling VIS versus OIS instrument effects..

Both Figures 11 and 12 show a distinct pattern where the strongest foEs values are present after a layer has descended to about 90-110 km but further discussion of the climatological morphology of Es is left to a separate report. The presentation in the right hand panel shows that the absence of foEs estimates at high heights and low frequencies in the left hand panel is a result of many of those observations being blanketed by normal E returns.

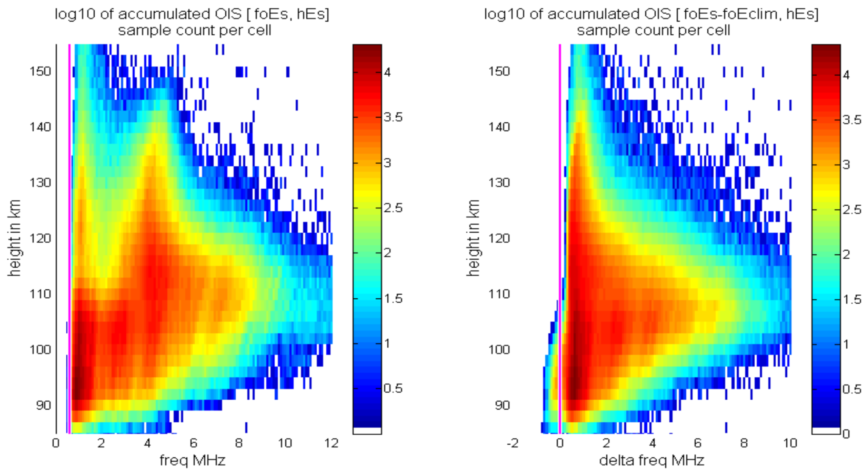

Figure 12 (a) A number density map of log10 of the binned sample count for foEs vs hEs data from all OIS sounder data from 2016 (b) the same data with the x axis changed to δfoEs where δfoEs = foEs-foEclim ie the foEs wrt the climatological model of normal E.

A similar fB model for OIS data is thus

fB (high)= max (0.6, foE_clim +gap) where the gap is typically 300 kHz (4c)
and
fB (low) = max (0.6, .9*fE_clim) (4d)

This estimation of fB is a necessary part of the foEs estimation but the exact model of fB is not critical. To complete the estimation of the distribution of foEs, all the measurements of foEs and the estimates of fB must be combined to produce a CDF in the fashion described in section 3. A typical result is presented below in Figure 13 for an area averaged group of samples at a single time. All observations have estimated fB values even if foEs is observed but the fB values are only used if foEs is unobserved or missing or zero. This means there is no longer a need for the regularisation term when an average or weighted average of foEs measurements is used to estimate the statistical distribution of foEs because the inclusion of fB values means the foEs algorithm always has some data.

The key to the area averaged foEs estimation model is the data and when the number of foEs measurements is low, the estimation of fB. The key to the spatially varying estimate of foEs at a particular site is also the spatial weight of influence of neighbouring points. For simplicity when understanding the model, the algorithm has adopted the same weighting functions as used for hEs when an estimate of the distribution of foEs is calculated. The regularisation model can still be used to produce a smooth foEs estimate a long way away from any data but that is not the focus of this paper at this time.

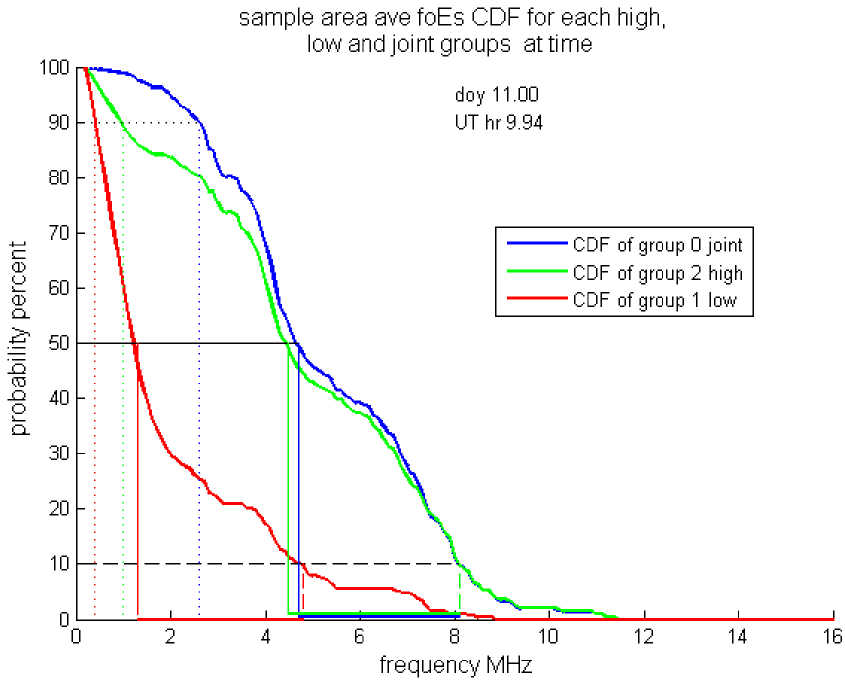

Figure 13 A plot of the CDF for each of the high (green) and low (red) and joint (blue) group of foEs samples at a single time in 2016 (total region accumulated groups of foEs samples).

Any single group of samples can be described by its CDF (for example Figure 13). This CDF can be described or summarised in many different ways (described in section 3). The climatological distribution of foEs can be described by producing maps of the probability foEs that will be above fixed frequency thresholds, for example, 3 or 5 or 7 MHz. But for the purposes of JORN the interest is in the frequency associated with a fixed likelihood. In Figure 13 the 3 representative likelihoods adopted are 10, 50 & 90% of the time/sample. In the following analysis, this paper focuses on the values of frequencies where the probability of foEs being observed has reached a critical number i.e. between 50 and 10% of the sample. f_p50 is the frequency of the median or 50th percentile (a good representative value of foEs) while f_p10 represents a plausible upper bound for a description of the distribution of foEs. Choosing 10% as a threshold allows the exclusion of the occasional extrema. The algorithm could have adopted 5% but when the sample set of measurements was small this makes the algorithm more vulnerable to outliers. A time series of the range of foEs values between 50 and 10% of samples are presented below in Figure 14 for each of the low, high or joint groups of foEs samples (accumulated over the entire domain) and below in Figure 15 for a weighted group of samples around a single particular location.

Described in this way, the important characteristics are f= f_p50 i.e. the frequency at any place and time when 50% of samples have foEs greater than this frequency and f=f_p10 i.e. the frequency at any place and time when less than 10% of samples have foEs greater than this frequency. In the range of frequencies f_p50-f_p10 sporadic E is said to be 'possible' i.e. possibly observed. In the range of frequencies f> f_p10 sporadic E is said to be 'unlikely'. In the range of frequencies f< f_p50 sporadic E is said to be 'likely'.

Figures 14 & 15 shows the change of f_p10 & f_p50 value from the CDF describing foEs as it varies over time for a number of days and for an area averaged description of foEs and a site specific case. The bottom panel of this presentation shows the number and ratio of non-zero foEs measurements within each of the separate layer groups.

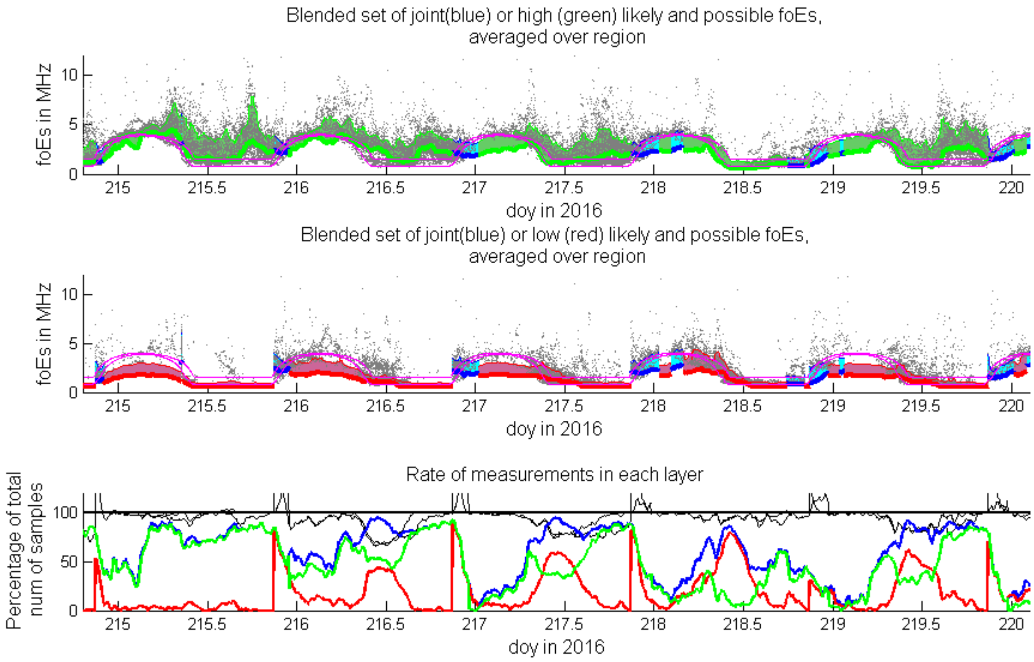

Figure 14   A time series plot of the properties of the distribution of foEs averaged over the entire domain (a) f_p50 & f_p10 and the maximum and median fB value for the high foEs or the common layer foEs depending on nL and (b) f_p50 & f_p10 and maximum and median fB value for the low foEs or the common layer foEs depending on nL and (c) the corresponding percent of non-zero total samples in each high, low or common group of samples.

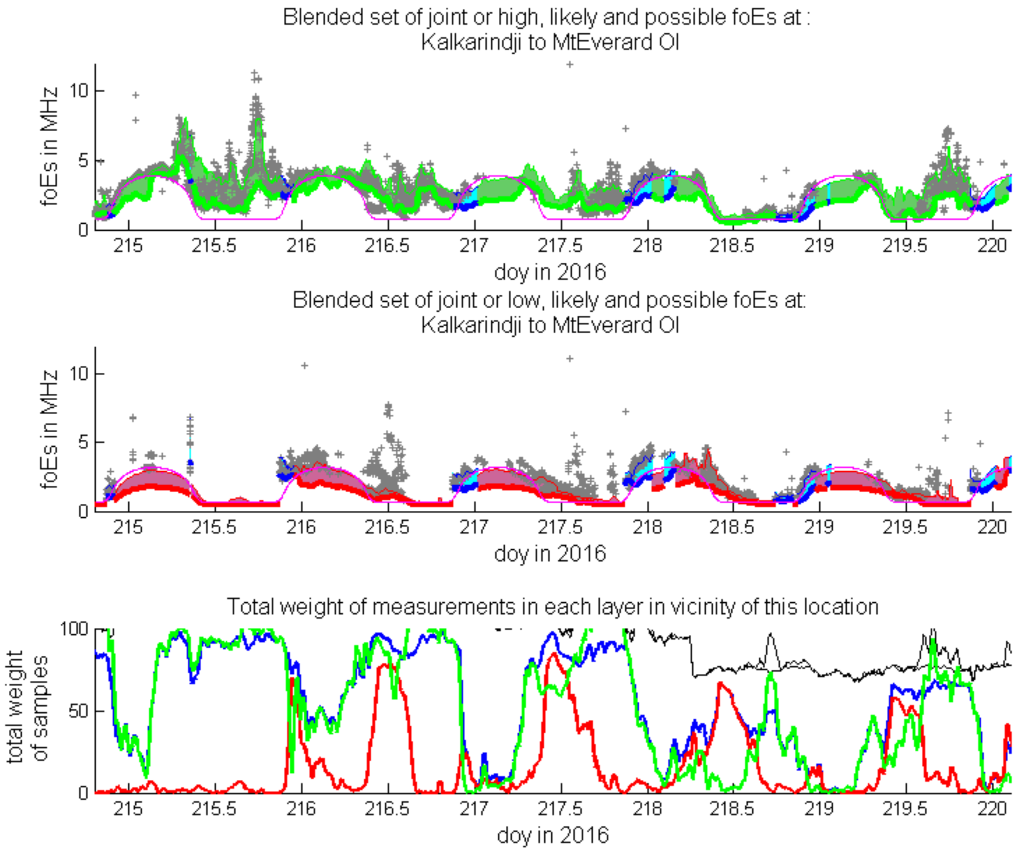

Figure 15 A time series plot of the properties of the distribution of foEs derived from data near a single OIS path (a) f_p50 & f_p10 and maximum and median fB value for the high foEs or the common layer foEs depending on nL and (b) f_p50 & f_p10 and maximum and median fB value for the low foEs or the common layer foEs depending on nL and (c) the corresponding percent of non-zero total samples in each high low or common group of samples.

It is worthwhile to note that in the bottom panels of Figures 14 the sum of the lower group and the upper group (foEs +fB counts) can be greater than 100% of the total number of samples because of the small overlap of the groups that is included to produce some stability. More-over in the bottom panel of Figure 15 it is visible that the number of upper group measurements can be greater than the total number of samples because sometimes an OIS produces two samples of Es and both those OIS Es samples from an image can come from the upper group of hEs (one strong return and one weaker return).

The spatial difference between the area averaged estimate of foEs in Figure 14 and the local estimate of foEs in Figure 15 is hard to visualise. A spatial distribution of estimates at a single time is presented below in Figure 16. This shows the spatial pattern of foEs (f_p50 &f_p10 only) in the Es layers at a single time. At this instant, and in this example, there is no significant low foEs to observe. It is worthwhile to note that the scale of the f_p10 values on the right hand side of Figure 16 has been stepped up 1.5 MHz from the scale of the f_p50 data on the left hand side. This means that areas where the colours match f_p10 = f_p50 + 1.5 MHz. Changes in the relative colour between left and right hand panels thus indicates more or less spread in the estimate of foEs. Regions where the weight of data contributing to the map has fallen below 16 samples have been left as foEs=0 (dark blue) just to show up the issue rather than relax the estimate toward the spatial average value and create better image continuity but hide the impact of diminished data availability.

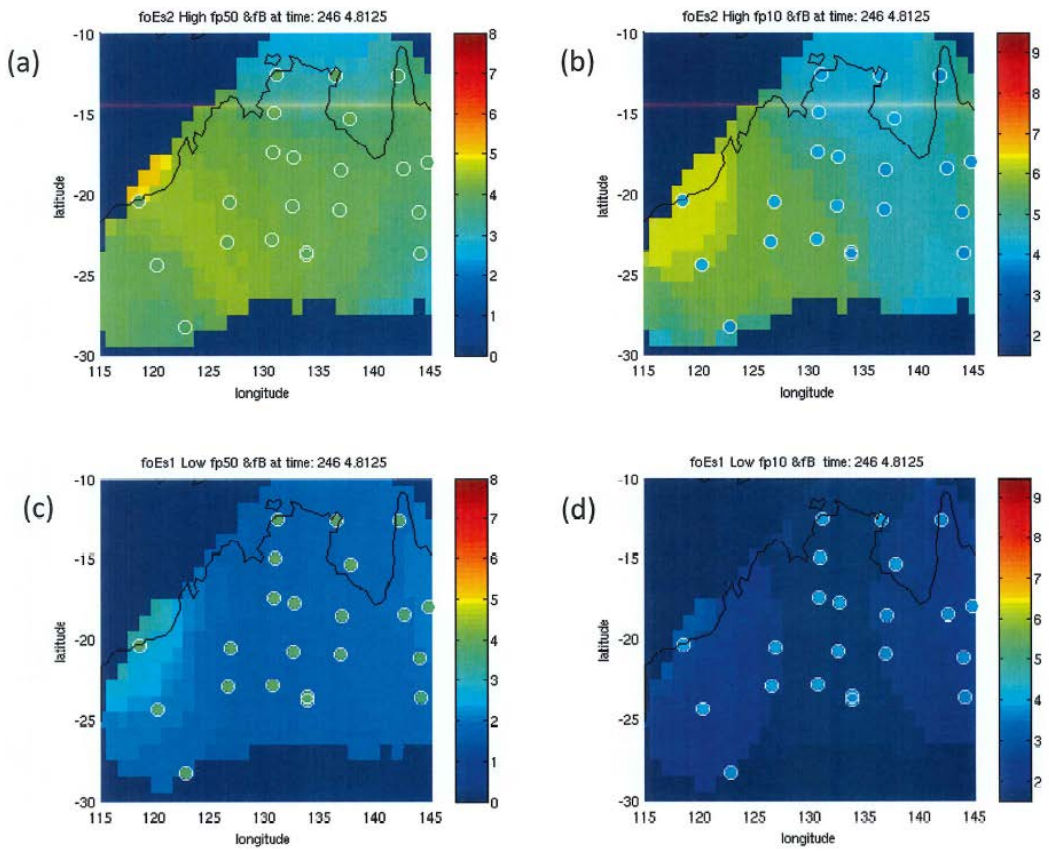

Figure 16 A single spatial map of foEs over the Australian region where panel (a) is the f_p50 value of the foEs high layer at a given location and (b) is the f_p10 value of the foEs high layer at a given location and (c) is the f_p50 value of the foEs of the low layer at a given location and (c) is the f_p10 value of the foEs low layer at a given location.The coloured dots on each panel are the mean fB values accumulated at each sites and included within the foEs estimate presented on the same colour scale as the main image.

This Figure shows the typical spatial variation and continuity that is present in the spatial maps of foEs properties. This continuity is largely due to the data making up a sample being accumulated over 30 minutes and 3 degrees while the sounder network sample rate is typically being 3.75 minutes in time and every 2.5 degrees.

4.4 BSS Es Trace Based Critical Frequency: foEs

The JORN Back Scatter Sounder system (BSS) represents an additional source of Es related observations of propagation to be exploited in support of Es modelling. The spatial sampling density of independent BSS observations is much greater than the sampling density of the combined VIS& OIS sounder network but the quality of the individual measurements is poorer. In particular it is worth-while to again note that the BSS Es information contains no direct information about the Es properties hEs or nL and it only has a potential to assist in the determination of foEs. This section of the report shows how BSS Es leading-edge trace information can be used to model foEs in the Australian region and discusses how similar and different this estimate is to the VIS& OIS based estimate of the previous section. The approach is to use the same algorithm as presented in the previous section but adapt the algorithm to the different nature of the available BSS inputs compared to the more direct and unambiguous VI and OI sounder measurements.

The first thing to note is that the JORN BSS traces are sampled approximately every 50 km of delay and in 8 separate beams of azimuth and with 4 different 90 degree radar segments. BSS image powers from delays of greater than 1800 km generally has very low elevation at sporadic E heights and hence seldom originate from Es. To focus on only using reliable data, BSS Es data from greater than 1800 km is excluded from the subsequent analysis. In addition signals from delays that are less than 900 km result from a much higher elevation and are frequently affected by meteor returns. To focus on automatic processing with a high reliability level, data with delays of less than 900 km is also excluded from subsequent analysis. This results in the use of BSS Es returns representing a narrow sample space (450 km of depth) in terms of the underlying geographic domain. This sample space is presented below in Figure 17

To enable an accumulation of samples to be used to characterise foEs a bounding interval around each a fixed set of geographic points is adopted. The algorithm adopts a range gate of +- 150 km (i.e. 5 samples in delay range) and an azimuth gate of +- 1 beam (i.e. 3 samples in azimuth) and 30 minutes of samples in time (i.e. 5-6 temporal updates). This typically accumulates data over a small region of < 2 degrees of latitude & longitude but the accumulation adds up to a useful number of sample measurements. An example of the BSS LE data that is typically available to be accumulated over a particular interval of time and space for one sector is presented below in Figure 18.

The previous OIS output started with Es measurements presented as Es characteristic vertical parameters [foEs, hEs]. The BSS processing starts with nominal oblique BSS LE information ie a MoF_Es for a given delay (range) and direction in the original oblique domain. With a mirror model of oblique propagation the Es oblique frequency can be related to the vertical Es frequency using Martyn's theorem (depending on the range and virtual height). This conversion factor can be calculated as a function of range and azimuth and the unknown virtual height.

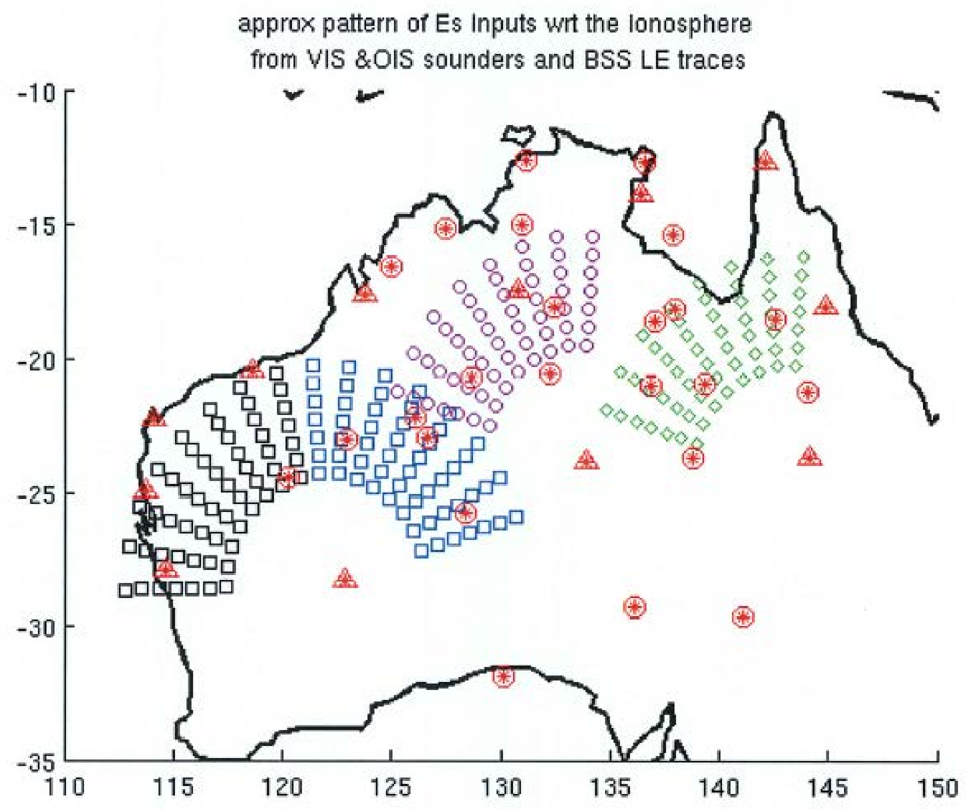

Figure 17 A geographic map of the nominal BSS beam and range sample points in addition to the VIS and OIS sample points in use for Es modelling.

All these factors can be combined into a single conversion factor or M_fact where

MoF_Es_obl = M_fact* foEs_est (5)

and the M_fact is a function of virtual height and range.

A plot of the M_fact as it depends on range and height is presented in Figure 19. For any range and azimuth a reference factor at a fixed nominal height (110 km) can be used to convert all the BSS oblique data within a sample into the vertical domain for all subsequent calculations. Measurement values based on this fixed height reference can be corrected to more correct values when the true height is known. This linear height dependent correction can be applied to all the reference data at a later stage of the processing when the correct virtual height to associate with the data has been established. The M_fact at a height of 110 is typically in the range 4-6whereas the final M_correction factor is presented in the right hand side of Figure 19 is much smaller than the original factor (< +- 25% of the reference vertical frequency). Never-the-less it will be important to keep track of this correction factor and the original range of the data.

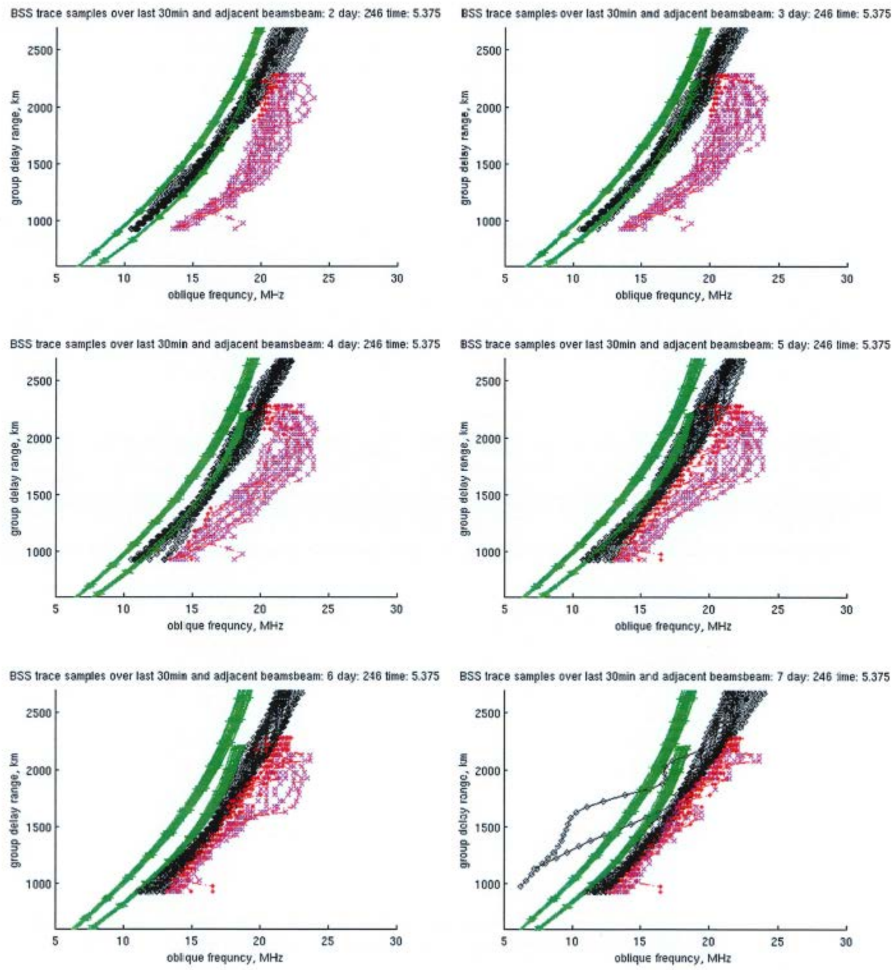

Figure 18 A display of a sample of BSS leading edges accumulated over the 6 centre beams and 30 minutes from R2 east. The E and F1 leading edges (from the model) are presented in green. The F2 leading edges from the BSS images are presented in black and the Es leading edges from the BSS images are presented in magenta. Red symbols are used to mark the BSS Es Leading edge information where the algorithm has marked the Es determination as dubious ie not clearly separate from other image features and hence status = 0.

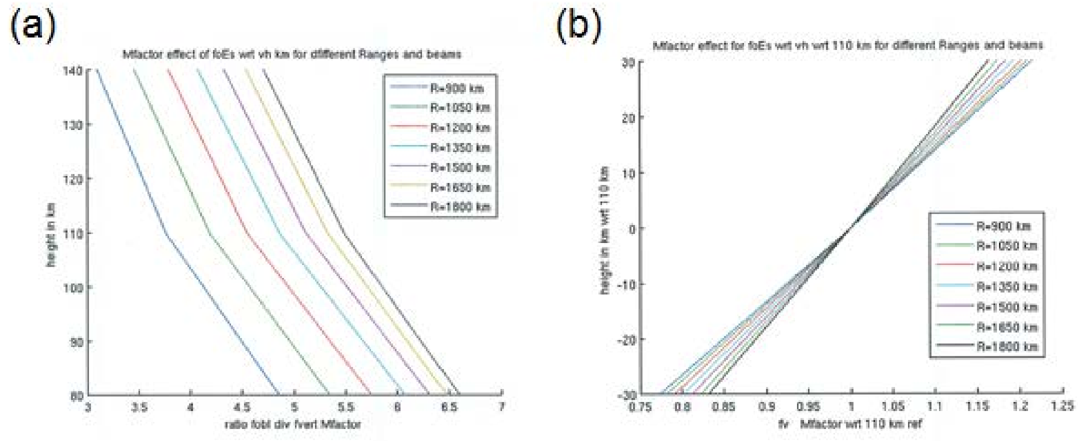

Figure 19 a) The height and range dependence of the oblique to vertical Mfact based on Martyn's theorem applied to Es heights and b) the percentage correction factor Mcorr over the same range but now referenced wrt the central nominal height ie 110 km

The previous OIS Es data processing used anomalous hEs values to identify and exclude outliers and bad data. In the case of the BSS Es samples the image processing algorithms label an Es trace with status > 0 (good) or status <=0 (extracted image value rated as potentially bad). While there are several reasons the Es trace could be labelled bad, the algorithm that has been adopted here chooses to apply the following conditions

IF Es trace (MUF_Es) >> the F trace observed AND

the status <= 0 THEN data is considered bad and weight = 0 (6a)

IF Es trace (MUF_Es) >> the F trace observed AND

the status > 0 THEN data is considered good and weight = 1 (6b)

Alternatively

IF Es trace (MUF_Es) ≈ F trace observed THEN
a separate Es observation is uncertain and an estimated fB value is used (6c)

Because some of the sounder observations are good but contain no Es it is necessary to estimate a notional fB value for each delay on the BSS image associated with the Es trace. The image oblique fB is recognised to be the maximum of the normal E, F1 and F2 returns observed from the BSS image (or the system model of it). This is converted to a nominal vertical fB using the same M_Fact as used for the foEs observation.

Thus with a nominal delay associated with a height of 110 km and the accumulation of good nearby BSS data the algorithms is now able to construct an estimate of the CDF that describes the BSS Es distribution. An example of the distribution of samples of BSS Es (and fB) at a single range and azimuth cell (assuming a constant reference height of 110 km) over a limited number of days is presented below in Figure 20.

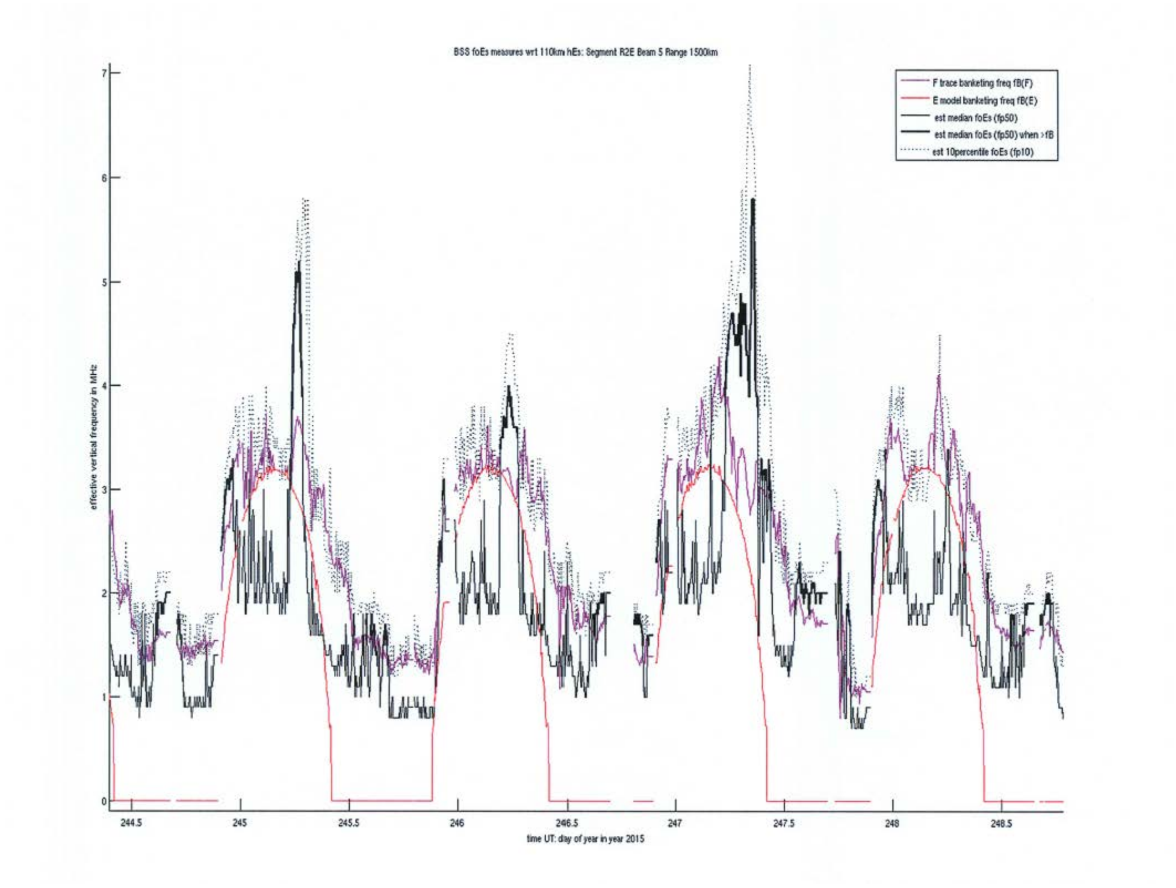

Figure 20 Example of BSS foEs and fB estimates based on the single reference Es height of 110 km from a single BSS sector, range and azimuth

This Figure shows the rapid changes present in the amplitude of Es at a given location and the variations that can occur when sometimes foEs is clear and numerous and observed in front of the BSS F returns and sometimes foEs is only intermittently in front of the BSS F leading edge and hence the estimated f_p50 for foEs is less than the BSS F trace fB value.

However, if these BSS foEs estimates are to be used in a model estimate of oblique propagation then they must have a height (nominally 110 km in the above Figure).

The next question addressed in this report is how to correct this foEs estimate to account for the choice of height derived in order to be consistent with the other VIS & OIS data.

Because the oblique BSS Es data is not available to be observed before it is in front of the oblique E MUF, observations of weak foEs very close to foE are rare. As a result of this and the data's oblique range the difference between vhEs and hEs in the determination of the foEs is not significant. As a result, the entire distribution of BSS foEs measurements can be scaled by a simple linear correction factor to present examples of the possible foEs distribution consistent with each of the three Es heights derived from the three separate hEs models (i.e. for hEs0ave, hEs1ave & hEs2ave). This means that when nL = 1 and the height hEs0 is known from the VIS & OIS observations of height then the correction that needs to be applied to the BSS data is clear. The question remaining is, how to associate the BSS returns with either the high or the low layer when the OIS data suggests nL =2 and both a high and a low layer have the potential to exist.

The BSS association algorithm adopted is to score each of the possible height associations based on a comparison with the VIS & OIS data foEs data. When the difference in score between the two layer alternatives is large then the choice is clear. When the comparative score is poor and or the difference is low then the choice is ambiguous (though for simplicity we have adopted the best match. The algorithms work on all data but the most important data is when the BSS f_p50 >fB. In those circumstances the BSS Es data is typically in front of the BSS F leading edge and hence the choice of layer height associated with the data is more critical. An example of the BSS foEs f_p50 data compared to nearby OIS foEs after a layer match has been made is presented below in Figure 21.

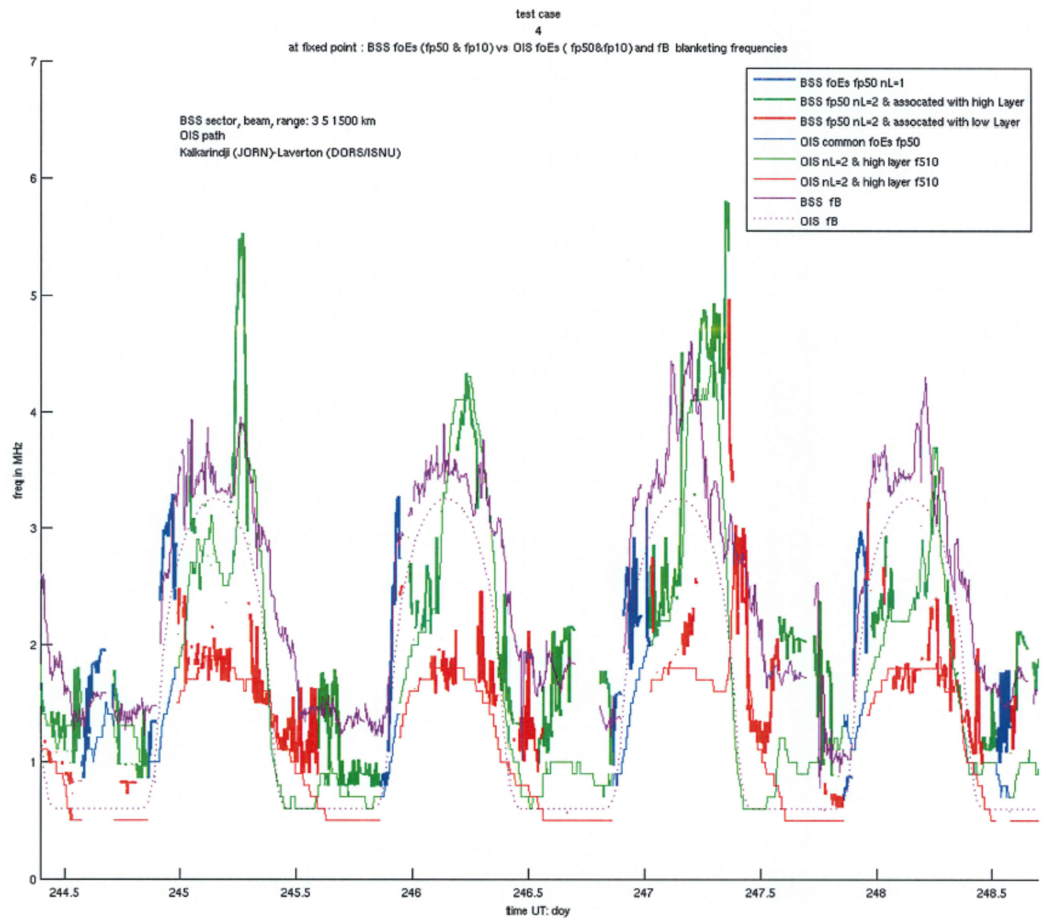

Figure 21 Example of BSS foEs f_p50 and fB estimates based on the Es height derived from the VIS & OIS data varying at a single point (BSS sector, range and azimuth) over time.

This algorithm shows how to use BSS trace information to estimate the distribution of foEs at any place and time in the Australian region (when the JORN BSS data is available). By the construction of overlapping samples of measurements the algorithm provides a parametric description of the distribution of foEs measurements that is smooth in space and time. The data in day 247 above shows the typical case where the BSS data is associated with the Es high layer (green) through the middle of the day but transitions to be associated with a growing low Es layer (red) as night falls. The consistency of these BSS derived observations of foEs with those derived from the VIS & OIS network covering the same space and time is described and discussed in a subsequent section of this report.

4.5 Path Loss and the Obscuration Frequency: fbEs

To date sounder processing has not been able to reliably or automatically extract fbEs estimates from the VIS and OIS images. This has meant that the algorithm has not been able to reassess or advance on results already published, see Sinno et al (1976), in order to update the systems model of fbEs based on new data. Never-the-less there is a need to have an estimate of fbEs for every estimate of foEs if oblique propagation loss is to be properly represented. The method of Barnes, 1995 could be applied to this data but to date a reliable estimate of obscured (diminished power) within the F returns has not been demonstrated.

It is proposed in this report to adopt a very simple model that is crudely consistent with the ideas of Sinno and the data and the previous modelling prior to a more thorough study being completed. In this new heuristic model it is observed that f_p50 is a representative value of foEs (50% of measurements have a value of foEs less than this whereas 50% will have a value greater than this) at any given time and location. Also f_p90 is a value of foEs that is so common (90% of measurements have a value of foEs less than this) that it could reasonably be assumed that the Es will block or blanket passing propagation when the critical frequency is below this value of foEs. Given the cloudy model of Es discussed earlier, this suggests that f_p90 would be a value at which only 10% of the cloudy region was clear and available for propagation to penetrate through to higher regions (the expected loss would be 10dB). The Sinno like rule used in the past was

$$fbEs = \alpha * foEs\_est \text{ where } \alpha \text{ is a fixed ratio eg } 0.55 \text{ or } 55\% \quad (7a)$$

The modification of this rule that adopted in this updated model is

$$fbEs = \max [f\_p90, \alpha * f\_p50] \quad (7b)$$

This has the desirable basic property of being roughly consistent with the past model and roughly consistent with the current data. It is expect that this model will be reviewed and revisited when more data becomes available.

5. A Description of Measures of Performance and Typical Results

5.1 hEs Measures of Performance

One purpose of the Es modelling is to create an accurate and smooth estimate of hEs. The questions are; How can this be quantified or measured? And How accurate and smooth is the particular model and algorithm that has been discussed?

A simple way of examining this is to adopt a representative set of measures or metrics and report the results of applying those metrics to a significant volume of real data. A direct measure of the accuracy of the estimate of hEs is the histogram of achieved values of σhEs i.e. the standard distribution of the fit to the data. Histograms of the results of this first metric applied to a years of VIS & OIS sounder data are presented below in Figure 22.

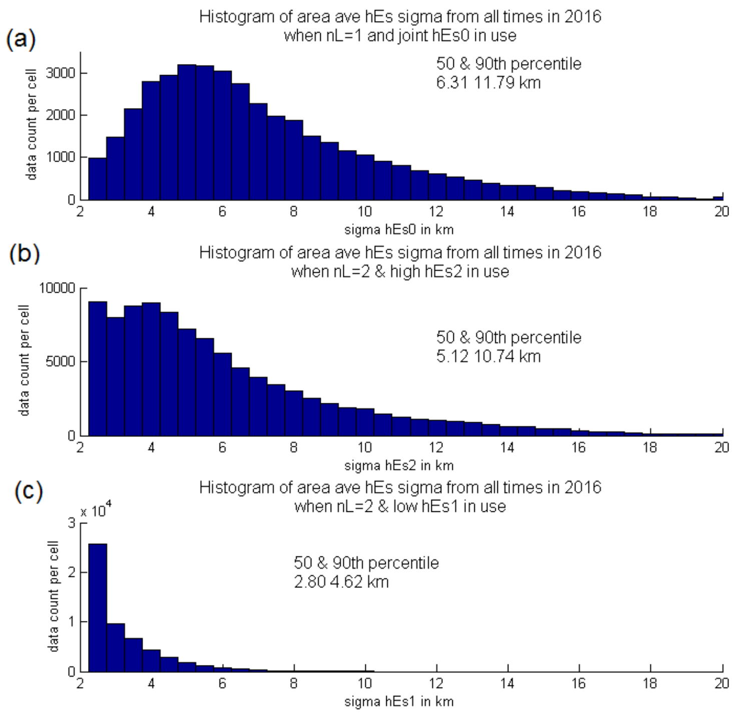

Figure 22 Histograms of the area averaged hEs estimate standard of deviation σhEs accumulated though 2016 as each estimate varies over time for each of the different hEs layers, when they occur a) σhEs when nL=1 for a joint hEs layer b) σhEs when nL=2 for a high layer hEs layer c) σhEs when nL=2 for a low layer hEs layer

These histograms of values can be reduced to a simple story by examining the 50th and 90th percentiles of the observed σhEs. This shows that the model of hEs typically has rootmean-square (rms) accuracy to within approximately 5 or 10 km for 50% or 90 % of the time respectively in the Australian region.

To break this down into greater detail the histograms of standard error in hEs can be accumulated on a per site basis (rather than an area averaged basis) or on a time of day basis. Examples of these patterns of accumulation are presented below in Figures 23 and 24

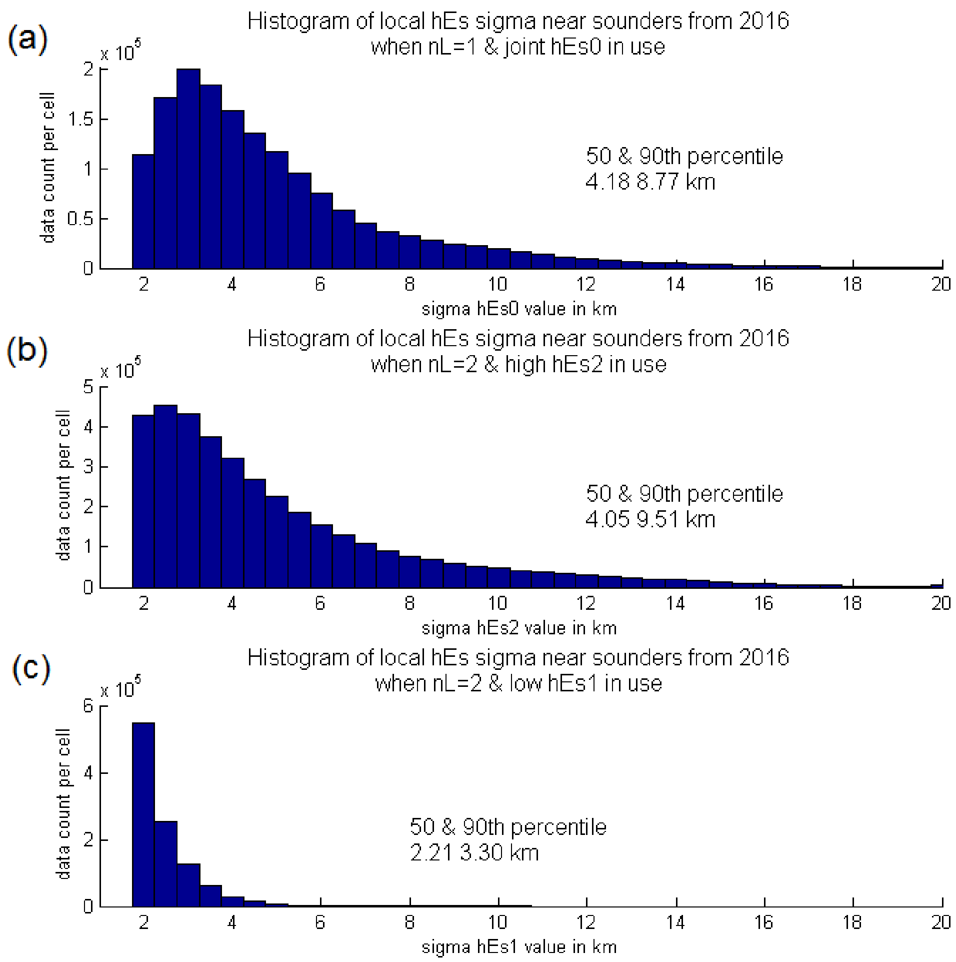

Figure 23 Histograms of the hEs estimated standard of deviation σhEs accumulated at each sounder site (47 separate sites) over the year of 2016 a) σhEs when nL=1 for a joint hEs layer b) σhEs when nL=2 for a high layer hEs layer c) σhEs when nL=2 for a low layer hEs layer

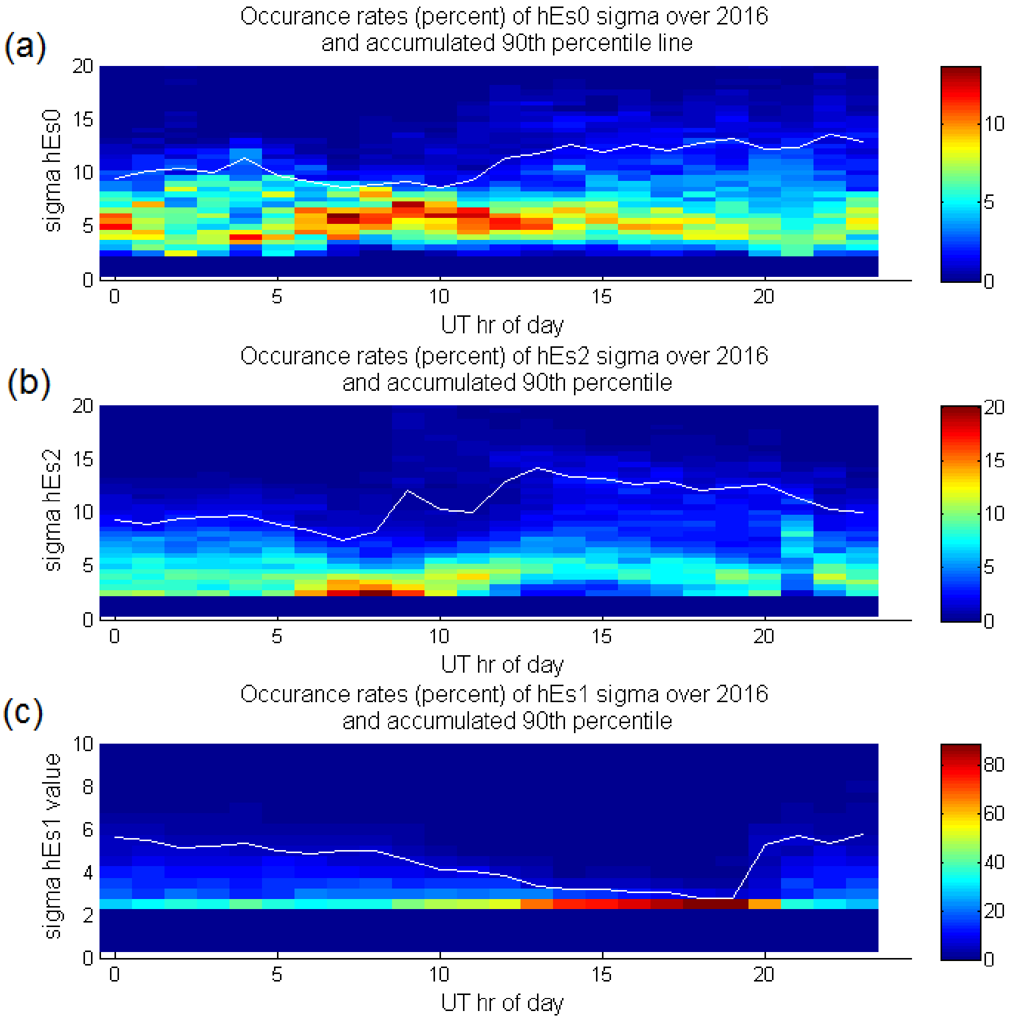

Figure 24 Histograms of the hEs area averaged estimate standard of deviation σhEs as it varies over UT time of day as a percentage count in each height bin a) σhEs when nL=1 for a joint hEs layer b) σhEs when nL=2 for a high layer hEs layer c) σhEs when nL=2 fora low layer hEs layer

The central conclusion of these measures is that there is a great deal of variability in the height of hEs and a greater deal of variability in the number of measurements that are routinely available. Despite this, the inaccuracy of the models estimate of hEs is much less variable and is typically < 5 km under normal conditions and, when conditions are hard and data is sparse, this sometimes grows to <10 km, for example, just before dawn. Additional analysis, not presented here, shows that this basic conclusion remains valid if the analysis is applied to different seasons and different ranges of amplitude i.e. values of foEs.

To address the question of the level of smoothness (in both space and time) within the hEs model a different set of measures and metrics are used. The normal variability of the hEs estimate in space can be observed by comparing local estimates of hEs with those of the area average. Histograms of the spatial delta hEs are presented below in Figure 25.

Alternatively histograms of the typical magnitude of change hEs over short periods of time (typically 7.5 minutes) are presented below in Figure 26. This gives some insight into the smooth nature of the hEs model particularly when change is scaled by the expected standard of deviation of the estimates.

Additional analysis, not presented here, shows that this basic conclusion remains valid if the analysis is applied to the local spatially separate measures of hEs or the spatial measures of hEs as a function of time.

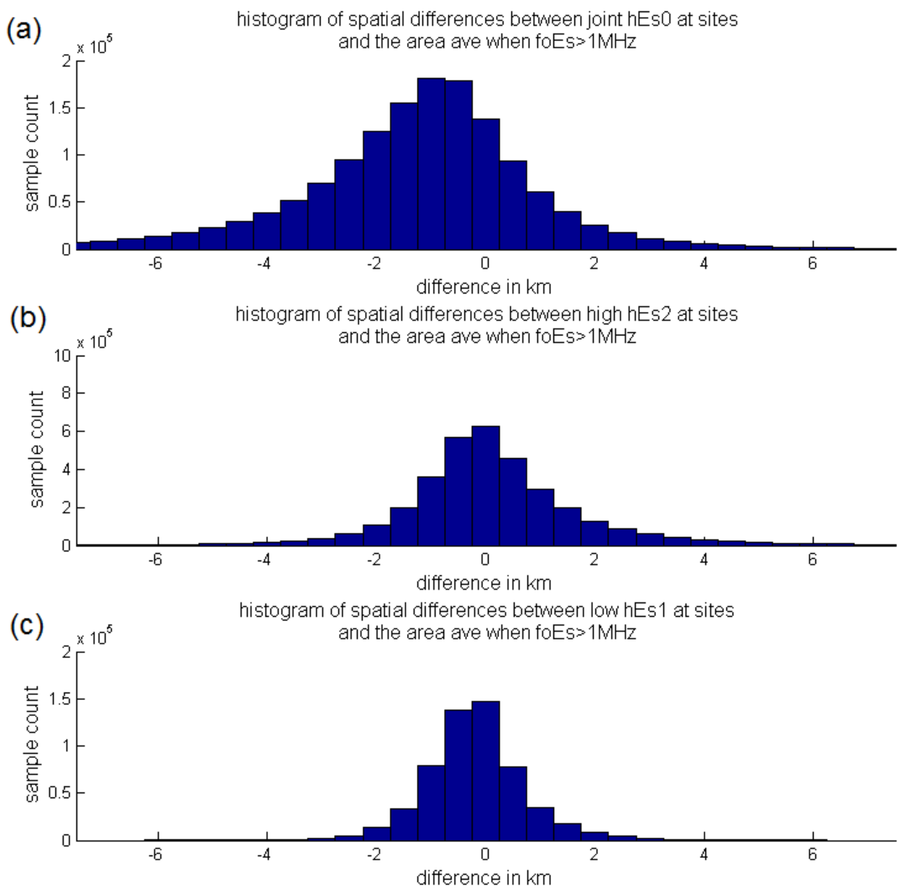

Figure 25 Histograms of the deviations between the estimated value of hEs at (47) sounder locations and the area averaged estimate of hEs accumulated over the year of 2016 a) when nL=1 for a common hEs layer b) when nL=2 and the layer data is from a high layer c) when nL=2 and the layer data is from a low layer

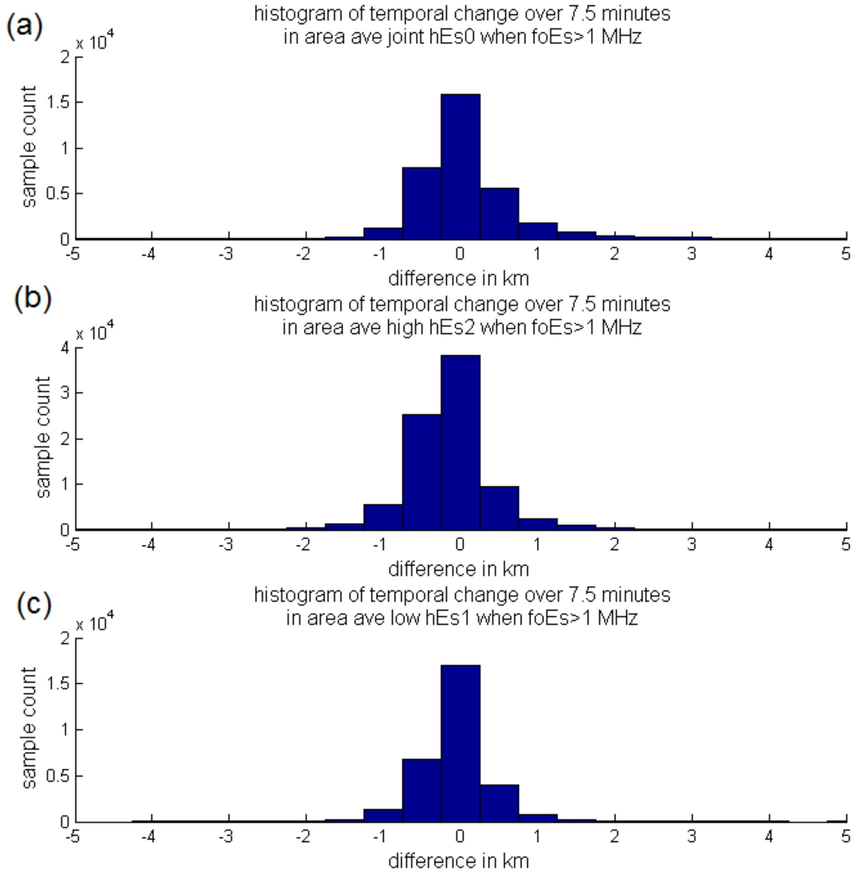

Figure 26 Histograms of the change in the area averaged hEs estimate over 7.5 minutes i.e. representing the rate of change of hEs over 2016 a) when nL=1 for a joint hEs layer b) when nL=2 and the layer data is from a high layer c) when nL=2 and the layer data is from a low layer

In Figure 26 a small bias is visible showing that the hEs layer height estimates are generally descending (i.e. they have negative rate of change) but this rate is typically quite small compared to the modelling sample rate and hence doesn't greatly affect the smoothness of the hEs estimate. All of these metrics and measures demonstrate that the proposed model of hEs is highly consistent with the underlying sounder data and is smoothly varying in both space and time (at least away from nL transitions). The behaviour of the estimates in the vicinity of nL transitions will be discussed later.

5.2 foEs Measures of Performance

A second purpose of the Es modelling is to create an accurate and smooth description of variations in the behaviour of foEs. The questions are again; How can this be quantified or measured? And How accurate and smooth is the particular model and algorithm that has been described?

Unlike hEs, how to measure and quantify the description of an arbitrary distribution for foEs is less well defined compared to the assumed Gaussian distribution for hEs. In the following, the frequency separation between f_p50 and f_p10 (frequency of the 50th percentile and frequency of th 10th percentile of the data sample) is used as a simple measure of the spread in the distribution (40% of the samples) used to describe foEs at a single place and time, that is, some measure of the cloudiness of the Es. The histograms produced when this metric is applied to a years of VIS & OIS sounder data from 2016 are presented below in Figure 27.

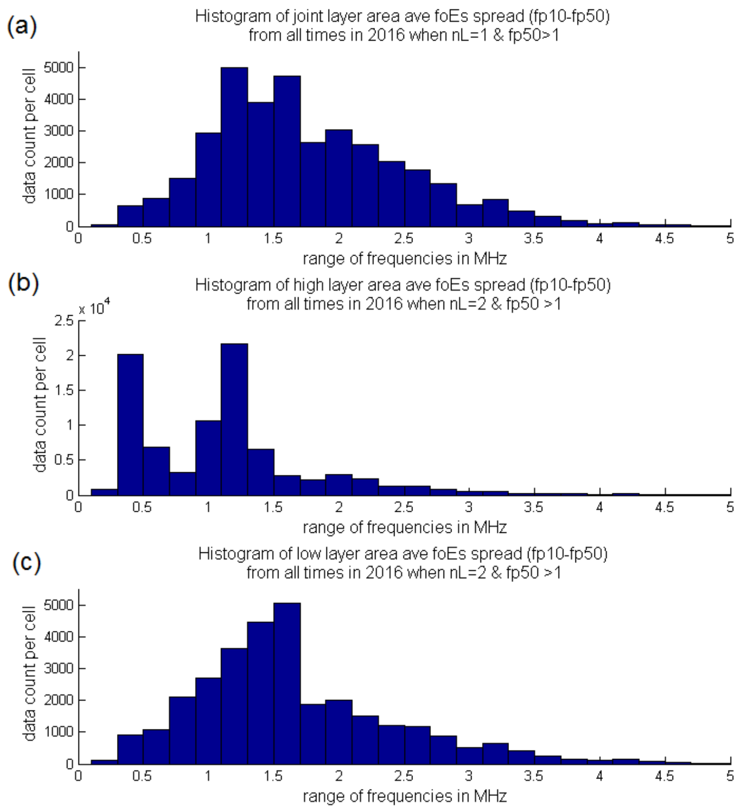

Figure 27 Histograms of the spread of the distribution of foEs ie f_p10-f_p50 accumulated though 2016 for the area averaged estimate of foEs as it varies over time for each of the different Es layers, when they occur. a) when nL=1 for a joint hEs layer b) when nL=2 and the layer data is from a high layer c) when nL=2 and the layer data is from a low layer.

These observations of the spread in the distribution of foEs can be reduced to a simple story by examining the 50th and 90th percentiles of the metric data. This shows that the model of foEs typically has a spread in the distribution of foEs that is between 1 and 3 MHz. This also shows that the lower layer Es (and the times when a joint layer is dominant) are much less numerous and more cloudy that the high layer returns at any typical instant in time. For a significant period of this the time the high layer foEs is quite tightly grouped (<0.5 MHz of spread) but the pattern is in many ways still sporadic.

To break this down into greater detail the histograms of the spread in the distribution of foEs can be accumulated on a per site basis (rather than an area averaged basis) or on a time of day basis or within a specific range of hEs or foEs values. Some examples of these patterns of accumulation are presented below in Figures 28 and 29.

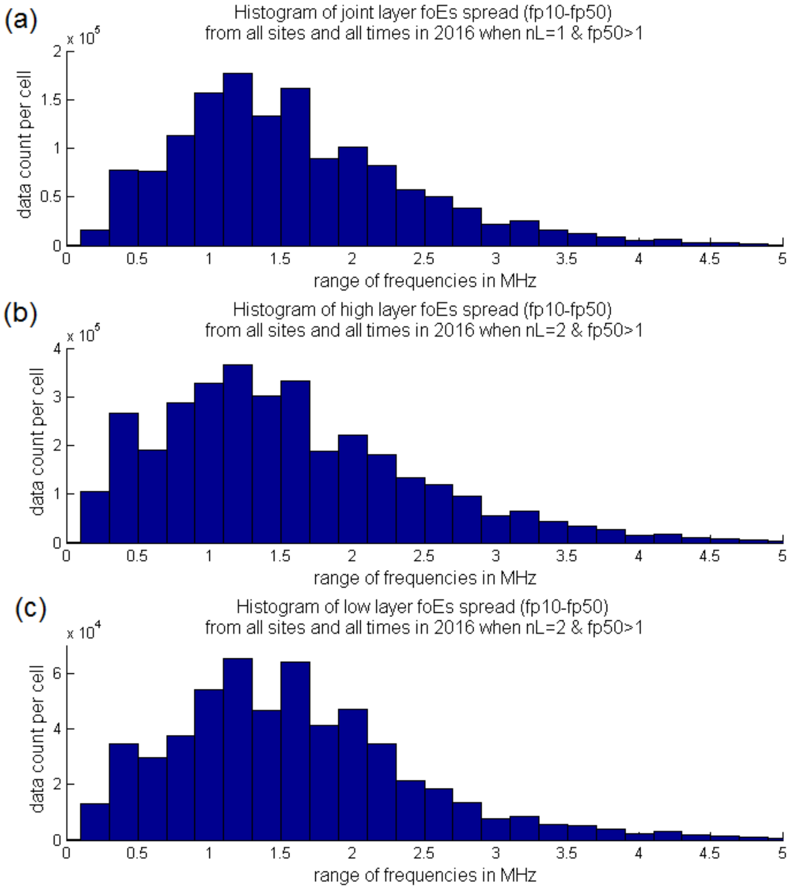

Figure 28 Histograms of the spread of the distribution of foEs ie f_p10-f_p50 accumulated though 2016 from all local site estimates of foEs as it varies over time for each of the different Es layers, when they occur. a) when nL=1 for a common hEs layer b) when nL=2 and the layer data is from a high layer c) when nL=2 and the layer data is from a low layer

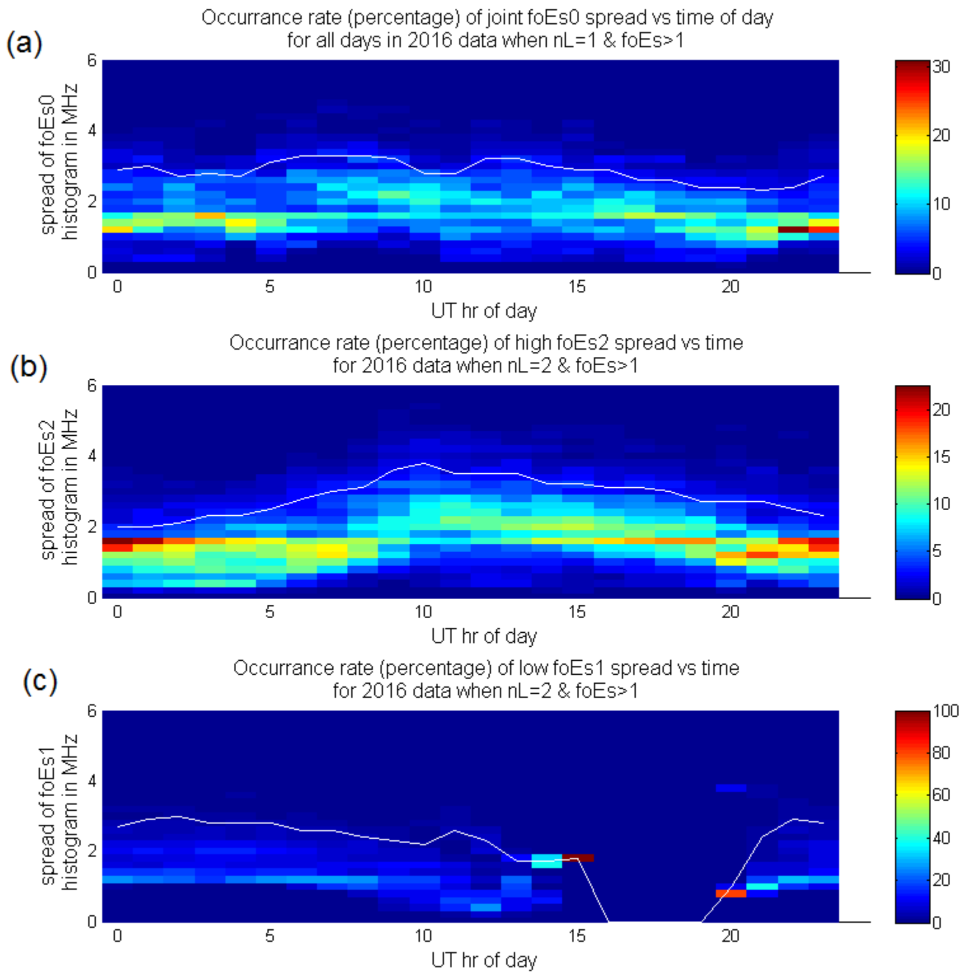

Figure 29 Histograms of the spread of foEs area averaged estimates as it varies over UT time of day. a) percentage of samples in a bin at a time when nL=1 for a joint Es layer b) percentage of samples in a bin at a time when nL=2 and the layer data is for a high Es layer c) percentage of samples in a bin at a time when nL=2 and the layer data is for a low Es layer. The white line is the where the accumulated position is less than 90% of the samples.

The central conclusion of these measures is that while there is a great deal of variability in the amplitude of foEs and a greater deal of variability in the number of measurements that are routinely available, the spread of foEs values within the distribution of foEs is much less variable and is typically in the range of 1-3 MHz. When external environmental conditions are good and the layer is high then this spread can often be <1 MHz but there will typically still be significant spread or cloudiness. While there is some pattern of diurnal variability in the spread of foEs and the per layer spread of foEs, the magnitude of differences in the spatial, temporal and seasonal pattern of variations is similar in scale to the basic spread in estimates at any single site and time. This is the reason Es is described as sporadic. Never-the-less , the general properties of foEs can still be characterised by smoothly varying parameters. While using the measure of spread f_p10-f_p50 is a somewhat arbitrarily selected heuristic, these Figures establish that, this measure is an informative and consistent numerical measure of the cloudiness of foEs. Additional analysis, not presented here, shows that this basic conclusion remains valid if the analysis is applied to different seasons and different ranges of amplitude.

To address the additional question of the degree of smoothness (in both space and time) within the characterisation of foEs a similar approach to the hEs metrics is adopted. The normal variability of the foEs parameter (f_p90, f_p50 and f_p10) estimate in space can be measured by comparing local estimates of parameters at a sounder site with those of the area average. Histograms of the accumulation of measurements of the spatial delta foEs created in this way are presented below in Figure 30.

Alternatively, histograms of the typical magnitude of change in foEs parameters (f_p90, f_p50 and f_p10) over short periods of time (typically 7.5 minutes) are presented below in Figure 31. This gives some insight into the smooth nature of the foEs properties within the Es model.

Additional analysis, not presented here, shows that the basic behaviour remains the same if the analysis is applied to the local spatially separate measures of foEs or the spatial measures of foEs are varied as a function of time.

Figure 30 shows that the spatial variation of a particular foEs characteristic, f_p50 at the 47 sample sites within the Australian region, is generally less than the spread in the distribution of foEs samples between f_p50 and f_p10. This is consistent with a commonly held picture of Es that when it is present it is wide spread though variations within the region are quiet large (i.e. of the order of 1 MHz). This Figure also shows that the spatial variation in a foEs characteristic, like f_p90, is smaller than the variations in f_p50 or f_p10 i.e. it is quite small and ≈ 0.2 MHz. This is consistent with a commonly held picture of Es that the base level of foEs is more persistently visible and wide spread and typically more spatially uniform than the peaks of foEs represented by f_p10.

All these Figures of foEs variation demonstrate that once the foEs cloudiness is characterised by a spread of parameters f_p90, f_p50 & f_p10 then each parameter in isolation is smoothly varying in space and time across the Australian region.

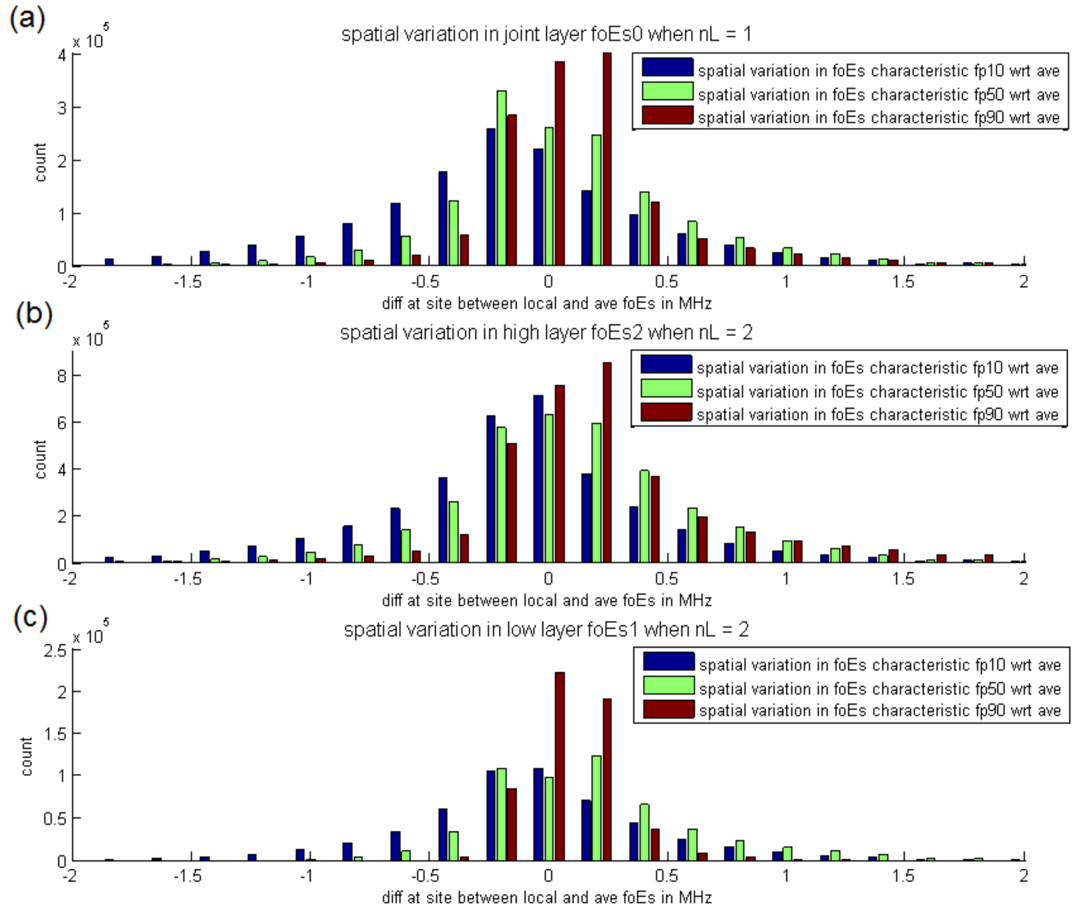

Figure 30 Histograms of the spatial delta in foEs properties f_p10, f_p50 and f_p90 (blue, green and brown) based on a sample of all sounder data from 2016, a) when nL=1 for a joint hEs layer b) when nL=2 and the layer data is from a high layer c) when nL=2 and the layer data is from a low layer

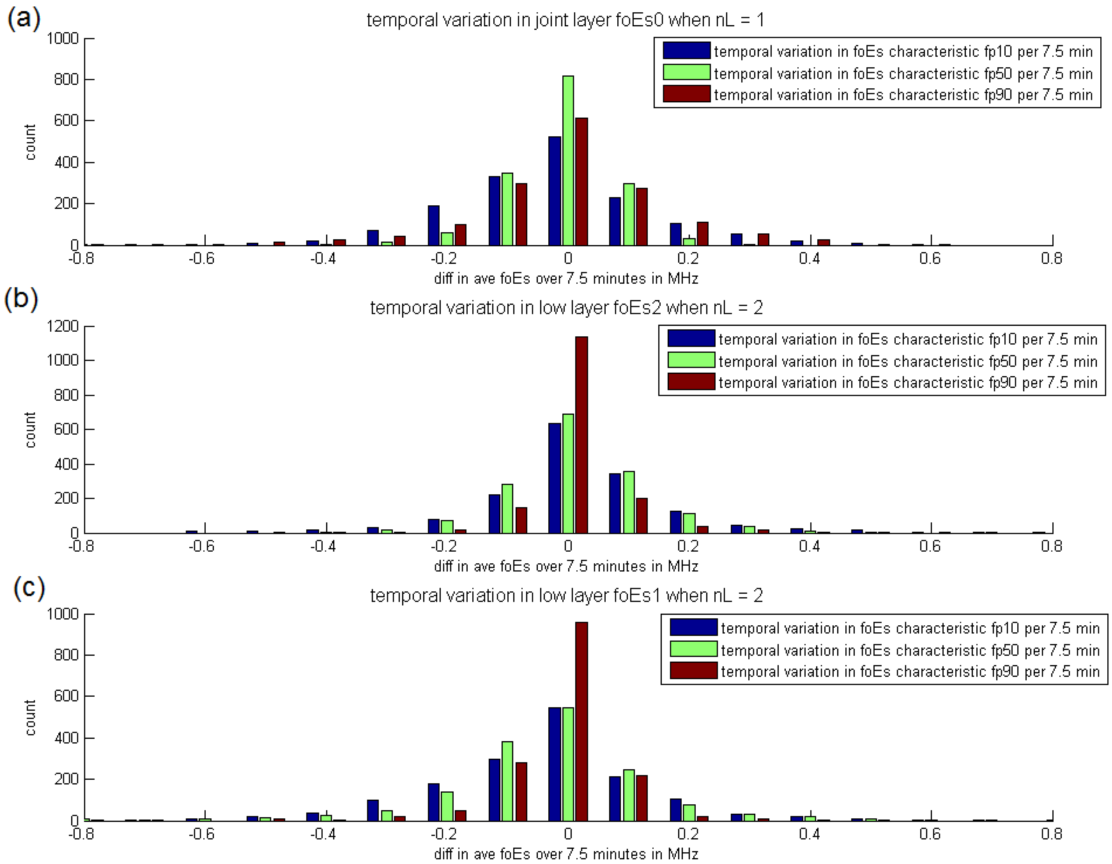

Figure 31 Histograms of the change of foEs characteristics (f_p10, f_p50 and f_p90) over a fixed time interval of 7.5 minutes (2 samples)for all times in 2016, a) when nL=1 for a joint hEs layer b) when nL=2 and the layer data is from a high layer c) when nL=2 and the layer data is from a low layer.

All of these metrics and measures demonstrate that the proposed model of foEs is highly consistent with the underlying sounder data and the parameters describing its distribution are smoothly varying in both space and time (at least away from nL transitions). The behaviour of the estimates in the vicinity of nL transitions will be discussed next.

5.3 Measures of Performance through nL Transitions

A significant concern regarding a model of Es is the reasonableness of the selected value of nL and establishing if there is expected to be frequent changes in the value of nL for unclear reasons. In the following section, this paper tries to show that, based on the algorithm adopted, changes in nL are typically simple to interpret and smooth in nature.

A test of the algorithms over an accumulation of all data from 2016 shows that the total number of changes in nL over the year was 1541 and the typical number of nL changes is about 4 (two up and two down) per day. The typical duration of a single nL=1 or nL=2 state is found to be 2 and 5 hours respectively. One of these nL changes typically occurs around dawn when the high low separation is very mixed in the Australian region and a single joint Es layer is the most common outcome (for a short period of time). A second change can typically occur at any hour depending on the data and the time of year. The pattern of these nL changes with respect to the time of day is presented below in Figure 32.

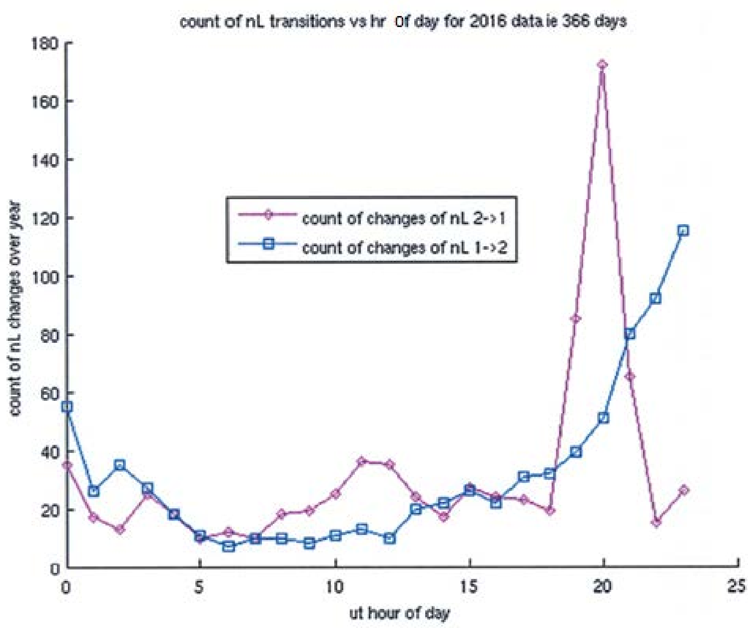

Figure 32 Histograms of the number of nL transitions as a function of time of day for transitions nL= 2->1 and nL=1-> 2 based on 366 days of data from 2016.

Detail analysis shows that an up-down change of nL within less than 1 hour is uncommon but not rare. The key measure sought is not the existence of a change in nL but establishing if there is a clear sense of Es continuity between one layer as nL changes. This continuity can be estimated by measuring the proximity of any new layer after an nL change with respect to the previous layer state, and scaling the height change by the estimate standard of deviation. Figure 33 below shows a single example of this proximity for a small sample of transitions within 2016.

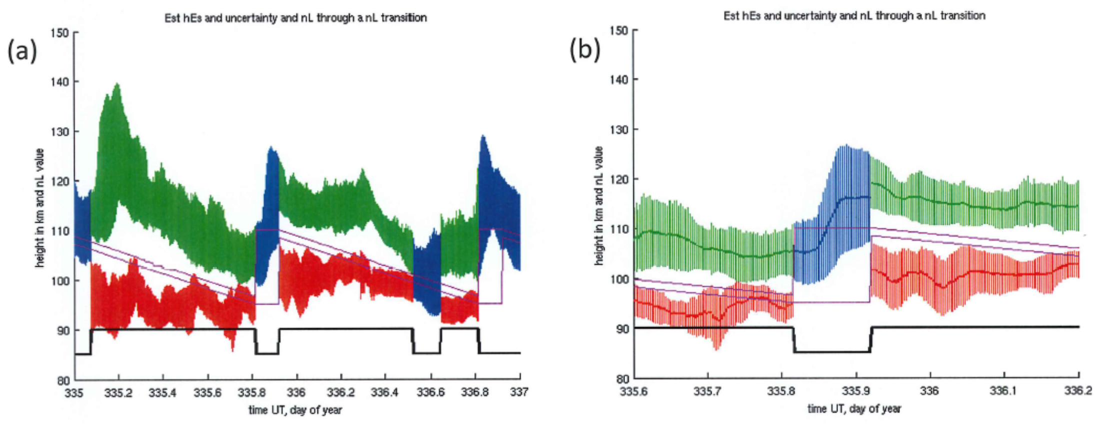

Figure 33 A time history plot of hEs mean height plus and minus one standard deviation over (a) a 3 day period of time and (b) the same data as panel (a) but with the time axis focused down around a single transition.

Any height change over an nL change can be measured in terms of the standard deviation of the estiamtes. A change of is less than one standard of deviation from the preceding layer estimate presents as a likely layer association across the nL change particularly if the other layer alternative association has a change of much greater than a single standard deviation. This pair of measures can produce a 'score' for a likely association over a change of nL. If the score is 'good' a before/after association can confidently (and automatically) be assigned.

Figure 34 shows this score of proximity over transitions within the year of 2016 where an association is defined to be 'good' if one association has a difference of less than one sigma and the other possible association has a much greater difference. Out of 1541 transitions this measure of 'score' results in 1430 transitions that can be made with confidence and are treated as unambiguous. The remaining 98 transitions are treated as ambiguous by the automatic assignment algorithms. 13 of these transitions have so little data and foEs <1 MHz so that an ambiguous or unambiguous transition is a 'moot point'. This leaves 85 transitions for the scrutiny of an operator over the 366 days of 2016. The majority of these transitions are high returns transitioning to a joint layer and then returning back to high layer in short order.

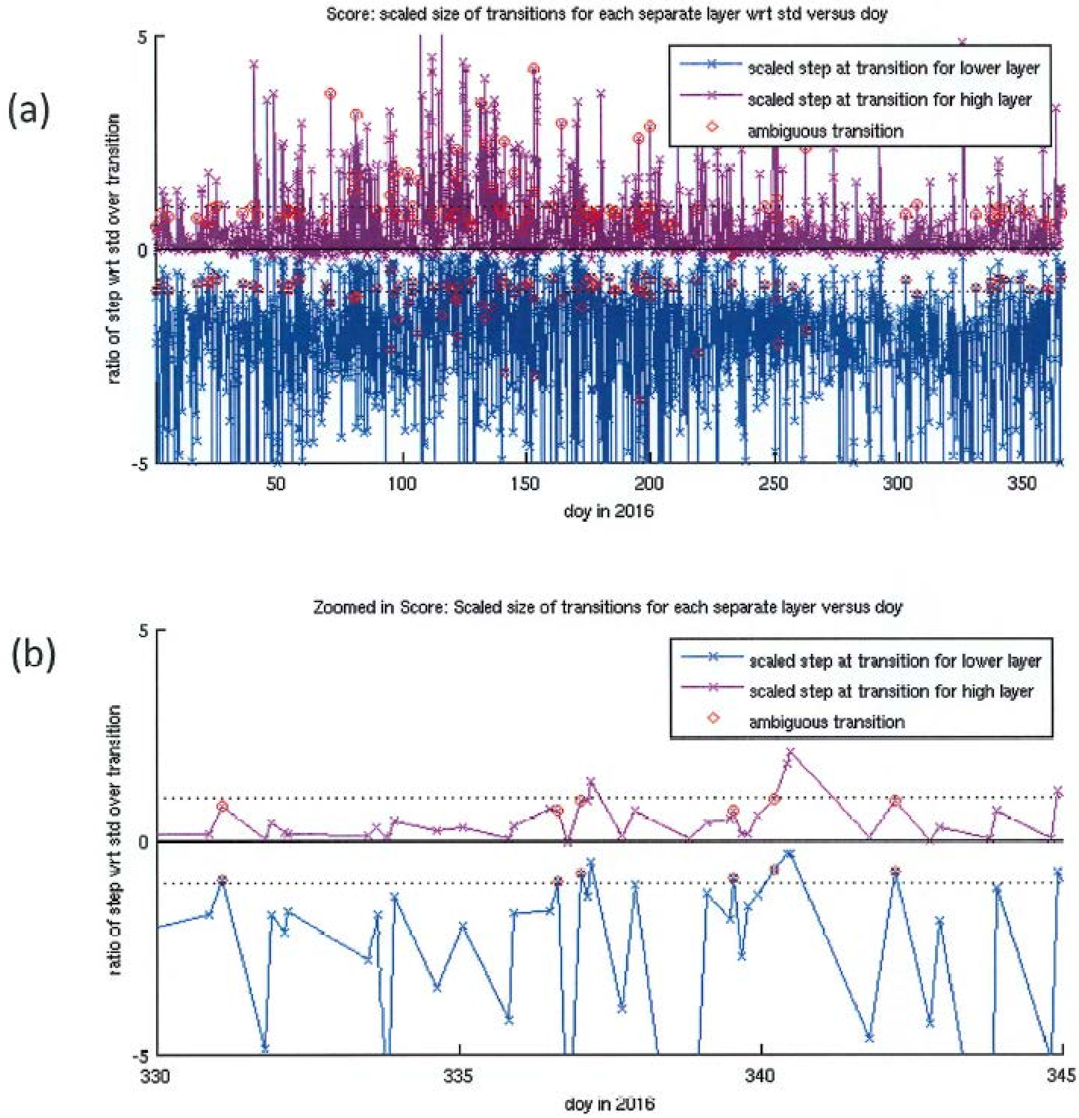

Figure 34 (a) A time series of the weighted hEs difference when nL transitions occur. The magenta line is transitions between high and joint layer estimated heights whereas the blue line is the weighted score between low layer estimates and the joint reference heights. Red symbols are over-plotted on the data that is estimated to be ambiguous i.e. no single layer transition is obviously preferred. Panel (b) is exactly the same data as panel (a) but zoomed in time to show a limited sample of 15 days (and 6 ambiguous transitions)

These Figures do not touch on the continuity observed in the foEs properties over nL transitions. The foEs continuity can be estimated by presenting the value of foEs property changes over nL transitions once hEs has been used to gain confidence in the associated layer label. This is presented below in Figure 35.

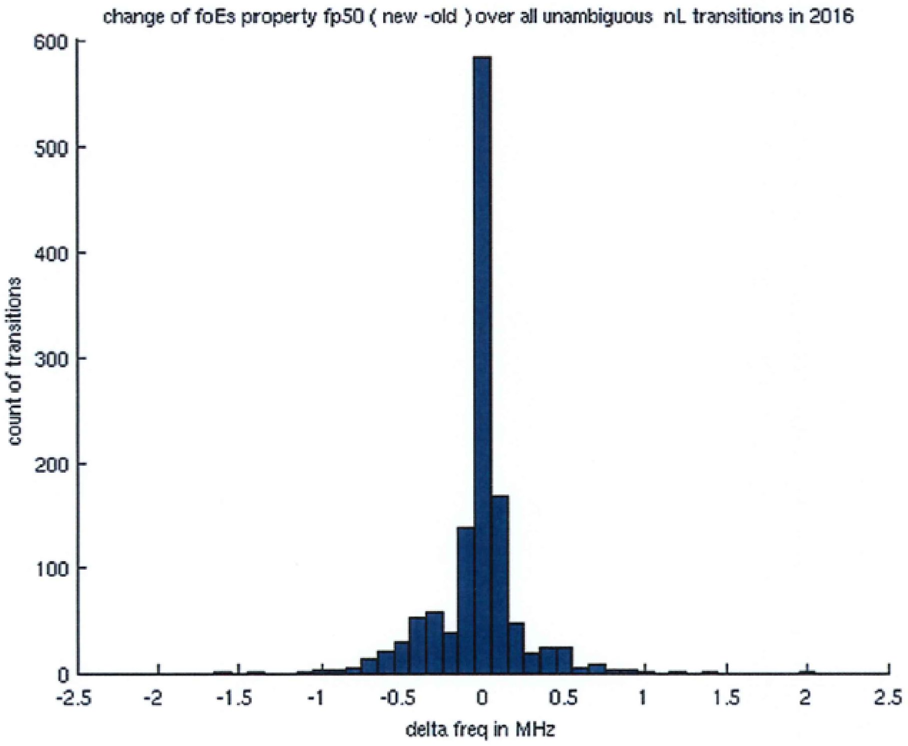

Figure 35   A histogram of the change in foEs property f_p50 over nL transitions in 2016.

This Figure shows that most of the transitions are smooth changes over time with foEs f_p50 changing by less than 0.5 MHz. This is slightly larger than the changes within a joint layer (presented above in Figure 31) but is still small enough to be within the typical f_p90->f_p10 edges of the distribution of foEs.

In summary, these results demonstrate that the Es properties are generally smooth over nL transitions from nL=1 to 2 or nL=2 to 1 with respect to the measured standard of deviation of the hEs parameter or the spread of foEs. This makes the automatic and parametric description of Es smooth and continuous and the multiple height models of Es is a complexity that is generally managed by the automatic association process over nL changes.

5.4 Measures of Consistency between BSS and VIS/OIS Estimates of foEs

To date the model of foEs generated from VIS & OIS data has been recorded separately from the similar model of foEs generated from BSS Es leading edge data even though the data covers the same space and time. To date only 30 days of BSS LE data has been available and tested and this is considered too limited to be confident of success if it was proposed to routinely integrate the BSS and the OIS data into a single common model. Also the 30 day period available is from August-September of 2015 when the seasonal cycle had a low occurrence rate for Es. Never-the-less this short period can be used to create a reference when defining a measure or metric to compare a sample of BSS foEs and a sample of OIS foEs estimates at the same place and time. To separate the comparison issues that are based on the core data processing from the associated height , in the first instance, the BSS foEs characteristics f_p50 and f_p10 are compared with the nearby OIS that is registered a single common layer . An example of a time series plot is presented below in Figure 36.

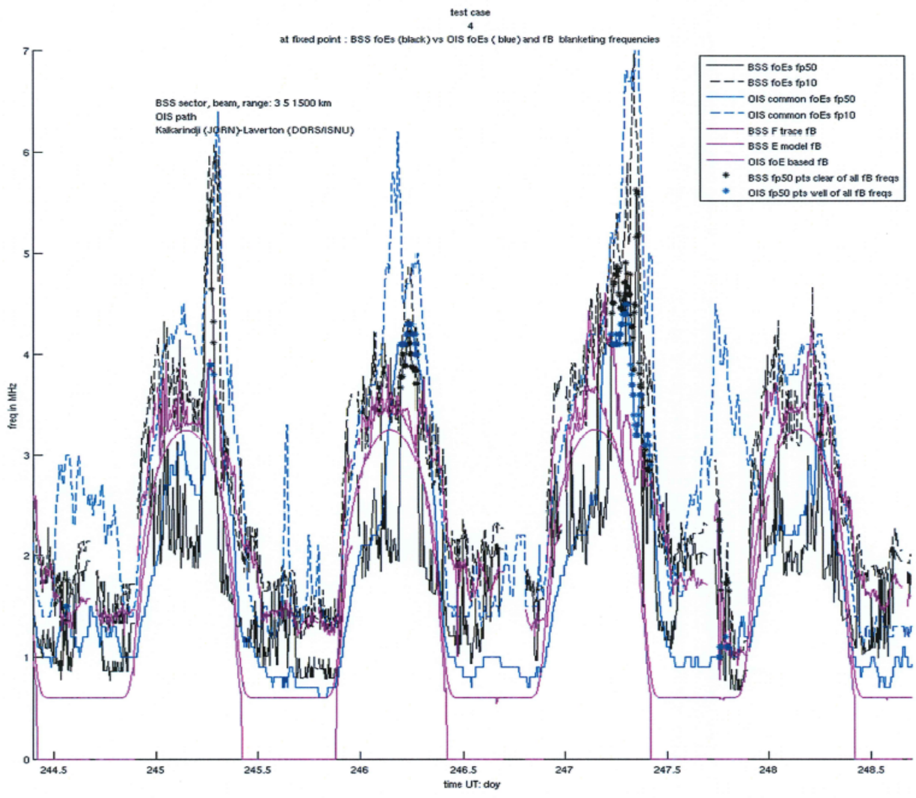

Figure 36   A time series of OIS versus BSS estimates of f_p50 and f_p10 over a period of time

To quantify the comparison, a histogram of the difference between the OIS f_p50 and the BSS f_p50 is produced below in Figure 37.

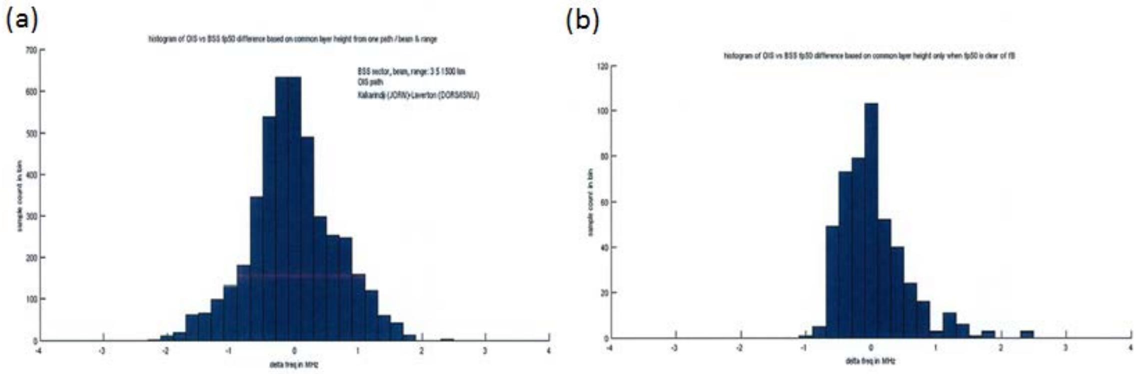

Figure 37 A time series of OIS versus BSS estimates of f_p50 and f_p10 over a period of time (a) for all samples and (b) for only those samples where f_p50>fB

While the size of this sample is to small to be definitive it is a common result to have the OIS and BSS foEs characteristics vary consistently (to less than 1-2 MHz) and to be more consistent when the measure f_p50 is greater than fB.

6. On the Management of the Human Machine Interface (HMI)

The main purpose of the operator interface is to enable the operators to manage the modelling decisions so that confidence in the model output is maintained. This section discusses how this is proposed to happen without giving the operators so much freedom that they can create an Es model that is unattached to the observed data that is usually used to support the model estimate.

The first simple functionality is related to nL and its changes. The HMI could present an opportunity to fix nL =1 so that the Es model will not change or flicker between nL=1 and 2. Fixing nL=1 will produce results similar to the historical model and these results would be very easy to understand and interpret. In the case when operators believe this very simple model is too inaccurate for their purposes, another form of this control could be to hold the nL value at either level (1 or 2) so that the number of layers is fixed into a pattern that the operator was happy (with rather than automatically let the system decide) i.e. set, nL= 1,2 or auto).

In the auto configuration (preferred) the previous results have suggested that most automatically induced changes have a strong sense of continuity i.e. it takes a big change of data to change nL from 1 to 2 (or vice-versa) and when there is a change the sense of continuity is clear. Never-the-less, there is a potential for an automatic algorithm to come to dubious decisions when the number of data samples is low. A new aspect of the HMI could present operators with an opportunity to accept and confirm any nL change decision or the layer before and after association over a change, for all nL changes or just some changes (eg the 98 cases that are assessed in some way to be more ambiguous). A more automatic system would call on operators only for ambiguous cases whereas a more manual system would call for an operator decision every time (typically 1-5 times per day).

A second simple functionality is related to the use the sounder data quality flags. Normally these show when a sample or two are outliers with respect to neighbours. Sometimes all data from a particular sounder site or path over a 30 minute period is bad. This condition could be used to alert an operator to flag that sounder as bad (and exclude it from the model processing). It is desirable for this functionality to be automatic because it would be a simple and minimalist way so that bad data can be excluded from the Es modelling. A similar alert could allow good sounder sites/information that was restored to use but not restored to processing because it has previously been excluded. The main goal of this functionality is to let the automatic assessment of good versus bad data to focus on the intermittently good or intermittently bad data and not have the algorithm have to routinely cope with persistent fundamental sounder failures.

A third simple functionality is to allow the spatial variation in the hEs and foEs estimation to be lost i.e. the model would everywhere report a spatially constant background value and distribution (equivalent to all weights always being set to 1). While this would most likely be for hEs alone and separately from foEs this would produce results that should be very easy to understand and interpret even if they are less accurate at any particular location. This could be a functionality applied to the high and low Es separately such that a typical pattern would be low hEs1 is reported as the spatially averaged value where-as high hEs2 has spatial variations.

A final functionality controlled by the HMI interface would be to control the mixing of the VIS & OIS based model of foEs and the BSS model of foEs derived from the BSS leading edges. To date, sufficient BSS data has not been tested to be assured that the image extraction algorithm for the Es Leading edge is highly reliable under all conditions. A simple rule available to an experienced operator could allow the Es model to be a mix of VIS& OIS and BSS data. An operator ability to set [0 1] or [1 0] i.e. all or nothing from a particular source (OIS vs BSS) depending on the operators preference is another possible HMI interface with the algorithm. The algorithm presented in the main body of this report presents separately the VIS & OIS model of foEs and the BSS model of foEs. It is suggested that the two separate models could be blended when f_p50_BSS > fB_BSS so the model takes advantage of the superior spatial sampling of the BSS only when it is clearly visible in front of the normal F leading edge. It is suggested that BSS foEs not be used (or blended into the model) when it is potentially degraded by obscuration behind the F leading edge. It should be a matter for future discussion if an operator HMI should include a simpler or a more complex set of alternative blends.

All these changes are envisaged to be real time options to manage the Es modelling process and they sit aside from some of the underlying algorithm configuration changes such as shortening the temporal accumulation period (from 30 minutes default to 10 or 15 minutes) or changing the accumulation spatial weight scale (from 3 degrees default down to 1 or 2 degrees).

7. Conclusions

This paper describes in detail an algorithm used to model sporadic E true height (hEs) based on automatically processed sounder data. This paper shows that hEs can routinely be estimated with a median σhEs < 5 km in the region of interest while the central value of hEs varies over a range from 80-140 km. The spatial and temporal changes in hEs are found to typically be small (< 5km) and slowly varying over a scale of 3 degrees and 7.5 minutes with respect to the model estimated standard of deviation. This means that except in those circumstances where the number of Es layers within the model (nL) changes from nL =1 to nL =2 (or visa-versa) the model of hEs created is smoothly changing and hence it represents a useful model.

In addition, this paper has shown that an association can be established that provides continuity of delay over changes nL=1-> 2 or nL=2 -> 1. The data shows that the hEs estimated changes are typically within one times the uncertainty σhEs estimates of the associated separate layers and generally (>90% of the time) an association is found to present an unambiguous choice. Despite its smoothness, this model is demonstrated to reliably represent periods and places where hEs descends (sometimes quite rapidly) as part of the normal geophysical variation associated with the morphology of Es height. This model also represents the start and end of the presence of particular layers of Es. In this way the model is very 'data driven' and reactive to the real time changes in the data. This suggests that this Es model of delay is suitable for use in the real time oblique propagation modelling used within JORN and the complexity introduced by allowing nL = 1or 2 can typically be automatically managed.

This paper also describes, in detail, an algorithm used to model the distribution of sporadic E amplitude (foEs). Two separate variants are described, one based on a network of automatically processed VIS and OIS sounder data and a second based on a network of automatically processed BSS LE data. Each of these has adopted the same description of foEs that is designed to describe the probability distribution of a set of foEs sample measurements at a given place and time rather than a single deterministic value. This approach is found to produce spatially and temporally smooth changes in the foEs characteristics that maintain a good match to the data. The foEs characteristics adopted (f_p90, f_p50 & f_p10) are demonstrated to be a good match to the data by their method of construction. These properties are also informative concerning the sporadic E conditions. Times and places when foEs is highly likely or highly unlikely can routinely be estimated. The typical spread of the distribution of foEs (f_p10-f_p50) is found to generally be in the range 1-3MHz. Together, all the elements of this model have reduced the large scatter in observations of [foEs ,hEs] down to a representation of sporadic E variability that is both smooth and consistent with the data. This model leaves very little of the observed parameter variability unexplained. This is encapsulated in Figure 38 below, which shows a summary of all the variability in VIS & OIS data from 2016 and the natural variability in data with respect to the corresponding model estimate.

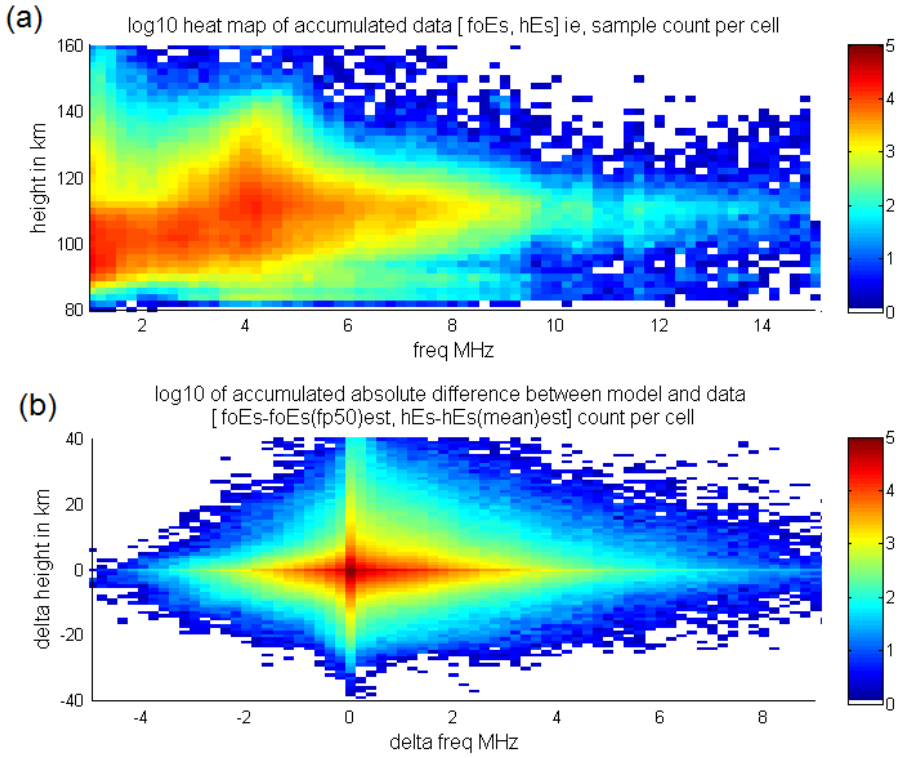

Figure 38 (a) Number density map of log10 of the binned sample count for foEs vs hEs data from all VIS &OIS sounder data from 2016 (b) the same data as panel (a) but with the x &y axis changed to represent the data binned w.r.t. to the model estimate i.e.

$foEs_{obs}$-$foEs_{median\ est}$ *vs* hEs_{obs}-$hEs_{mean\ est}$

In the top panel, the variation of all the hEs and foEs observations is clearly visible. The bottom panel contains all the same data but the image has counted the number density of the difference between the observations and the model representation of the data proposed in bins of the same size. This shows the considerable contraction in the uncertainty produced by using the model. It is worthwhile to note that this Figure shows log10 of the count of samples such that the scale 5 = 100,000 observations per cell and a scale of 3 = 1000 observations per cell.

The cross consistency between the OIS measure of foEs and the BSS measure of foEs (measured independently) is additional good evidence that the model of foEs adopted is real and a useful basis to describe what the Radar observes. While more analysis of BSS and Radar measurements of Es are required and desirable it is proposed that this type of modelling approach be adopted in any future model of Es within JORN.

8. Acknowledgements

The author wishes to thank and acknowledge the members of HFR Branch responsible for the routine generation and organisation of the processed sounder data used in this analysis. In particular thanks go to Andrew Heitmann, David Netherway, Brett Northey and Michael Whitington. The author also wishes to thank and acknowledge the many JORN maintainers. Without these people's diligence and effort this analysis would not have been possible.

9. References

1. Davies, K., 1990: 'Ionospheric Radio', Peter Peregrinus.

2. Kelley, M.C., 1989: 'The earths ionosphere: Plasma Physics and electrodynamics' Academic Press.

3. Mathews, J.D., 1998: 'Sporadic E: current views and recent progress', JASTP **60** 413-435

4. Barnes, R.I., 1995: 'Analysis of Es traces from a calibrated oblique ionosonde', JATP **57** 1753-1761

5. Smith, E.K., 1978: 'Temperate zone sporadic E maps', Radio Science **13** 571-575

6. Haldoupis, C., Pancheva, D., and Mitchell , 2004: 'A study of tidal and planetary periodicities present in mid-latitude sporadic E layers' JGR 109

7. Haldoupis,C ., Meek C. Christakis Pancheva, Bourdillion , 2004: 'Ionogram height – time-intensity observations of descending Sporadic E layers at mid-latitudes' JASTP

8. Haldoupis,C, 2012: 'Mid-latitude Sporadic E. A Typical Paradigm of Atmospheric-Ionosphere Coupling' Space Sci Rev **168** 441-461

9. Sinno, K., Kan, M., and Hirukawa, Y., 1976: 'On the reflection and transmission losses for ionospheric radio wave propagation via Sporadic E' Journal of Radio Research Laboratories **23** 65-84

DISTRIBUTION LIST

A Description of a New Model of Sporadic E for JORN

Robert Gardiner-Garden

Task Sponsor

Sponsor Name/ Position

S&T Program

Chief of Division, NSID
Research Leader: Dr Gordon Frazer
Task Leader: Dr Sam Davey

Dr Mike Turley
Dr Trevor Harris
Dr Robert Gardiner-Garden

DEFENCE SCIENCE AND TECHNOLOGY GROUP
DOCUMENT CONTROL DATA

1. DLM/CAVEAT (OF DOCUMENT)

2. TITLE

A Description of a New Model of Sporadic E for JORN

3. SECURITY CLASSIFICATION (FOR UNCLASSIFIED LIMITED RELEASE USE (U/L) NEXT TO DOCUMENT CLASSIFICATION)

Document	(U)
Title	(U)
Abstract	(U)

4. AUTHOR(S)

Robert S. Gardiner-Garden

5. CORPORATE AUTHOR

Defence Science and Technology Group
PO Box 1500
Edinburgh SA 5111

6a. DST GROUP NUMBER	6b. AR NUMBER	6c. TYPE OF REPORT	7. DOCUMENT DATE
DST-Group-TR-3443	AR-017-062	Technical Report	December 2017

8. OBJECTIVE ID	9.TASK NUMBER	10.TASK SPONSOR
	AIR 17/550	OC WASS SPO

11. MSTC	12. STC
High Frequency Radar	Geophysical Phenomena and Performance Assessment (GPPA)

13. DOWNGRADING/DELIMITING INSTRUCTIONS	14. RELEASE AUTHORITY
	Chief, National Security and ISR Division

15. SECONDARY RELEASE STATEMENT OF THIS DOCUMENT

Approved for public release

OVERSEAS ENQUIRIES OUTSIDE STATED LIMITATIONS SHOULD BE REFERRED THROUGH DOCUMENT EXCHANGE, PO BOX 1500, EDINBURGH, SA 5111

16. DELIBERATE ANNOUNCEMENT

No limitations

17. CITATION IN OTHER DOCUMENTS

Yes

18. RESEARCH LIBRARY THESAURUS

Ionospheric modelling, High frequency radio propagation, High frequency radar

19. ABSTRACT

The morphology and physics of Sporadic E (Es) differs greatly to the normal physics of other ionospheric layers, so it is generally treated and modelled differently. The Es model within the Jindalee Operational Radar Network (JORN) is a real-time model with values based on sounder data, and has essentially remained unchanged since JORN's delivery in 2003 (despite years of progress in sounder processing). While this model can be used to manage the system when Es is present, systemic model difficulties must often be overcome by the manual intervention of experienced operators. This paper describes a new fully automatic data driven real-time model of the morphology of Es, and describes the associated expected propagation characteristic that should reduce the need for manual intervention. It has been adapted to work with JORN ionospheric sounder data in real time and tested with years of data. The models performance is characterised and discussed, and a probabilistic cumulative distribution function (CDF) to describe the probable value of the amplitude of Es i.e.is constructed. It includes an algorithm based on the available sounder data to determine the number of separate Es layers present in the data and a recommendation is made for the new model approach to Es be adopted in any future enhancement of JORN's model of Es propagation.